

Boosting Multimodal Reasoning with MCTS-Automated Structured Thinking

Jinyang Wu¹ Mingkuan Feng¹ Shuai Zhang¹ Ruihan Jin¹ Feihu Che² Zengqi Wen² Jianhua Tao^{1,2}

Abstract

Multimodal large language models (MLLMs) exhibit impressive capabilities but still face challenges in complex visual reasoning. While recent efforts attempt to enhance MLLMs’ reasoning by incorporating OpenAI o1-like structured thinking through explicit search structures or teacher-guided distillation, they often struggle to balance performance and efficiency. A critical limitation is their heavy reliance on extensive data and search spaces, resulting in low-efficiency implicit insight extraction and data utilization. To address this, we propose AStar, an Automated Structured thinking paradigm for multimodal reasoning via Monte Carlo Tree Search (MCTS). AStar automatically derives high-level cognitive reasoning patterns from limited data using MCTS-powered hierarchical structures. Building on these explicit patterns, we design a unified reasoning framework that seamlessly integrates models’ internal reasoning capabilities and external reasoning guidelines, enabling efficient inference with minimal tree iterations. This novel paradigm strikes a compelling balance between performance and efficiency. Extensive experiments demonstrate AStar’s effectiveness, achieving superior accuracy (54.0%) on the MathVerse benchmark with a 7B backbone, surpassing GPT-4o (50.2%) while maintaining substantial data and computational efficiency.

1. Introduction

Multimodal Large Language Models (MLLMs) have demonstrated impressive capabilities across diverse tasks and domains (Yin et al., 2023; OpenAI, 2024; Chen et al., 2024c), such as autonomous driving (Cui et al., 2024), and visual question answering (Hartsock & Rasool, 2024). Their proficiency in complex multimodal reasoning, particularly in

*Equal contribution ¹Department of Automation, Tsinghua University, Beijing, China ²Beijing National Research Center for Information Science and Technology, Beijing, China. Correspondence to: Shuai Zhang <zhang_shuai@mail.tsinghua.edu.cn>, Jianhua Tao <jhtaoo@tsinghua.edu.cn>.

Preprint

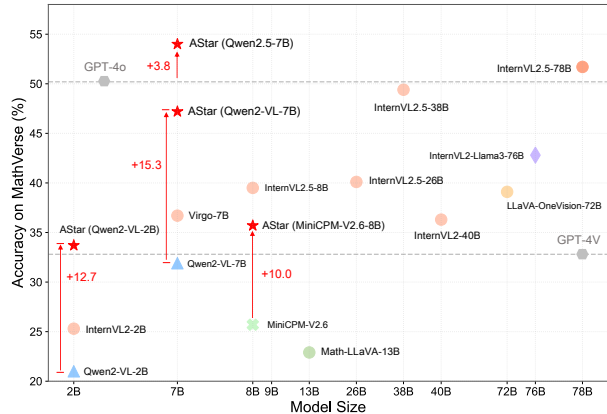


Figure 1. Performance comparison on the MathVerse benchmark. Our AStar framework achieves competitive results against most open-sourced MLLMs and closed-source ones, showing outstanding structured thinking and reasoning abilities.

mathematical tasks involving visual content, has emerged as a critical benchmark for evaluating fundamental cognitive abilities towards strong artificial intelligence (Searle, 1980; Goertzel & Pennachin, 2007; Wang et al., 2024f; Qiao et al., 2024). Mastering multi-step visual reasoning requires the integration of multimodal information, along with rigorous adherence to complex rules and sophisticated problem-solving strategies, presenting significant challenges for existing MLLMs (Zhang et al., 2024g; Wang et al., 2024a).

Inspired by recent advances in System 2 slow-thinking reasoning systems like OpenAI o1 (OpenAI, 2024) and QVQ (Team, 2024), there is growing interest in incorporating structured thinking into MLLMs (Xu et al., 2024; Dong et al., 2024d; Du et al., 2025). This direction aims to address the limitations of conventional MLLMs that often rely on simple ‘direct prediction’ modes due to the scarcity of high-quality long-chain reasoning data (Xu et al., 2024; Luo et al., 2025). According to existing literature, two primary approaches have emerged for implementing slow-thinking reasoning systems: explicit search and teacher supervision-guided training. The first approach leverages explicit search structures (e.g., Monte Carlo tree search, MCTS) with specialized reward models to guide the exploration of solution paths (Dong et al., 2024a; Yao et al., 2024). The second approach focuses on distilling structured reasoning patterns

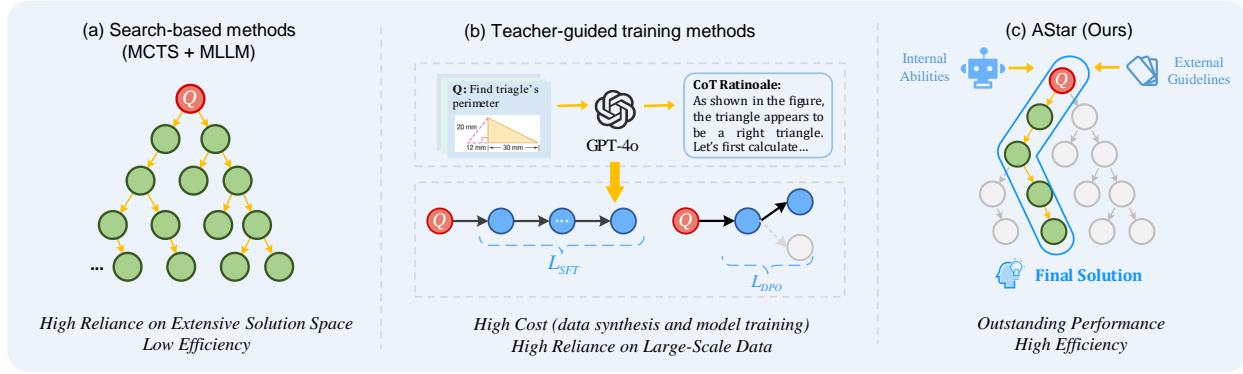


Figure 2. Schematic comparison between AStar and two mainstream structured reasoning methods. $\mathcal{L}_{(\cdot)}$ denotes the training optimization objective. (a) Search-based methods suffer from computational inefficiency due to extensive solution space iterations. (b) Teacher-guided training optimizes models using distilled rationales from powerful models like GPT-4o, but requires substantial data and computational resources, resulting in low-efficiency pattern extraction and poor data utilization. (c) Our approach effectively combines MLLMs’ internal implicit reasoning capabilities with explicitly extracted insights, achieving a compelling balance between performance and efficiency.

through long-form Chain-of-Thought (CoT) (Wei et al., 2022; Zhang et al., 2024g; Luo et al., 2025) instruction data, typically requiring supervision from closed-source models like GPT-4o for data synthesis.

Despite these advances, current reasoning paradigms face three critical limitations (Figure 2). First, search-based methods (Dong et al., 2024a) suffer from computational inefficiency due to extensive solution space iterations. Second, teacher-guided training methods (Hu et al., 2024; Yao et al., 2024; Luo et al., 2025) typically require substantial training data ($\geq 100K$) and computational resources to implicitly extract reasoning patterns, resulting in low efficiency and poor data utilization. They also heavily depend on proprietary models like GPT-4o for data synthesis, making them impractical for researchers outside major enterprises. Third, static and predefined reasoning processes (Xu et al., 2024; Thawakar et al., 2025) constrain flexibility, leaving the reasoning potential of MLLMs underexplored.

To address these challenges, we propose AStar, an Automated Structured Thinking paradigm for multimodal Reasoning via MCTS. Our approach introduces a novel mechanism for automatically deriving high-level cognitive reasoning patterns from limited data (500 samples) using MCTS-powered hierarchical structures (aiming to address the second limitation). Building on these explicit patterns, we design a unified reasoning framework that seamlessly integrates internal and external advantageous attributes, enabling efficient adaptive inference with minimal tree iterations, thereby tackling the first and third limitations. *This novel reasoning paradigm effectively combines MLLMs’ internal implicit reasoning capabilities with external explicit reasoning guidelines, achieving a compelling balance between performance and efficiency.*

Specifically, our method comprises three steps: (1) visual reasoning action definition, (2) MCTS-powered thought card construction, and (3) adaptive reasoning and verification. *First*, we define six atomic reasoning actions as building blocks of chain-structured reasoning patterns (termed “thought cards” that serve as reference insights during inference). These actions simulate human-like cognitive behaviors, including problem decomposition and reasoning step reflection. *Second*, using a small seed dataset (500 samples), we apply MCTS to derive reference reasoning patterns to construct multiple thought cards. *Finally*, in the reasoning stage, we select the five optimal thought cards most aligned with the target problem’s cognitive complexity. With these reasoning guidelines, we perform visual reasoning and validate the final solutions via self-consistency checks or outcome reward models. Experiments demonstrate that AStar exhibits impressive reasoning performance with enhanced efficiency, comparable to powerful closed-source models like GPT-4o (Figure 1). Our main contributions are:

- **Automated Reasoning Paradigm:** proposing an MCTS-based automated approach for generating and selecting the optimal reasoning patterns.
- **Efficient Action-Chain Guided Reasoning:** providing explicit guidance for each step of the visual reasoning process, enhancing structured thinking capabilities.
- **Superior Performance:** achieving 54.0% score on the challenging MathVerse benchmark with a 7B backbone, surpassing GPT-4o (50.2%).
- **Improved Efficiency:** achieving comparable performance to recent tree-based methods while reducing inference overhead by $6.4\times$, and matching training-based methods while requiring $520\times$ less prior data.

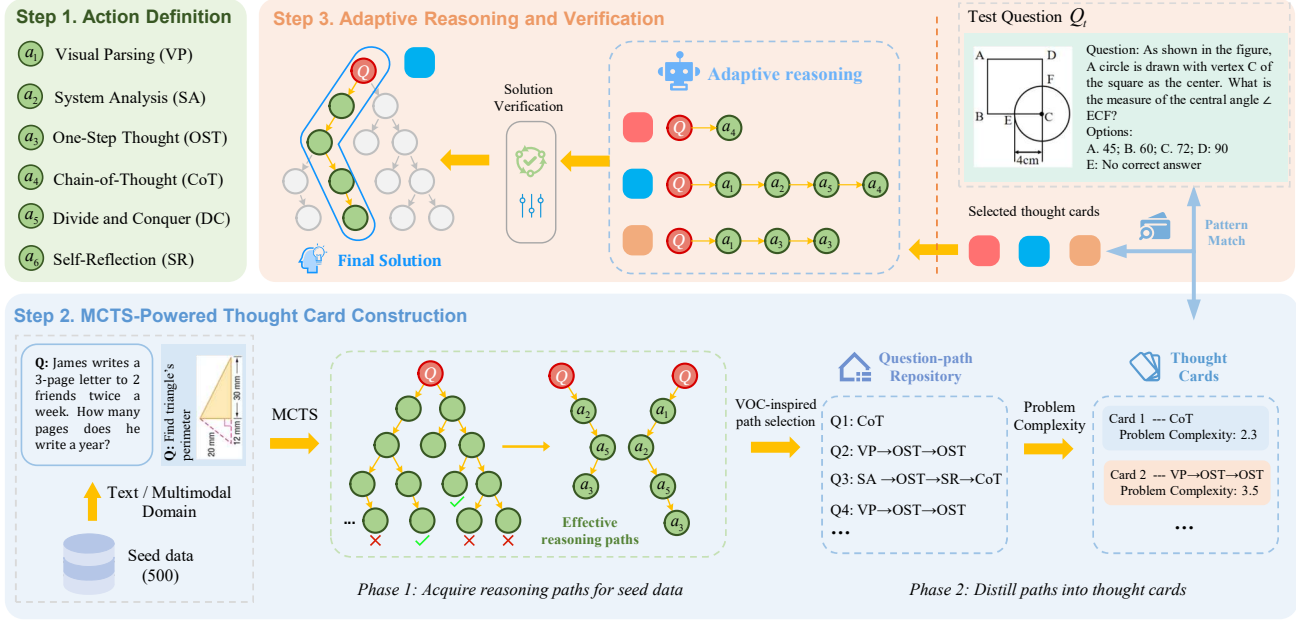


Figure 3. Flowchart of our proposed method AStar. This framework consists of three main parts: (1) Visual Atomic Reasoning Action Definition; (2) MCTS-Powered Thought Card Construction; (3) Adaptive Reasoning and Verification.

2. Related Work

Multimodal Reasoning Recent advancements in MLLMs have demonstrated robust capabilities across diverse domains, including visual understanding (Zhang et al., 2024c), mathematics (Zhang et al., 2024d; Du et al., 2025), and scientific inquiries (Zong & Qiu, 2024). Despite these achievements, complex multimodal reasoning remains challenging due to its demands on both visual perception and high-level cognition. Inspired by OpenAI o1’s impressive performance, recent approaches (Zhang et al., 2024e; Xu et al., 2024; Thawakar et al., 2025) attempt structured reasoning with pre-defined stages, enhancing MLLMs’ CoT capabilities (Zhang et al., 2024g). However, their rigid structure limits flexibility across different tasks, overlooking the importance of adaptive reasoning in unleashing multimodal reasoning potential (Wang et al., 2024e). Our approach addresses this by introducing a hierarchical tree structure that enables task-specific reasoning path generation and selection.

Tree-based Search Tree structures have demonstrated significant potential in language models (Zhang et al., 2024a; Qi et al., 2024; Wu et al., 2024a). Recent efforts explore applying these tree search methods to search effective reasoning paths for MLLMs. While AR-MCTS (Dong et al., 2024a) enhances multimodal reasoning by integrating MCTS with active retrieval, its extensive iteration requirements and computational overhead limit practical applications. Similarly, Mulberry (Yao et al., 2024) leverages tree structures to distill 260K long-chain reasoning data

from powerful models like GPT-4o, but requires substantial computational resources and high-capacity teacher models. These methods struggle to achieve an optimal balance between performance and efficiency. To address these limitations, we propose incorporating high-level reasoning abstractions into MCTS, achieving competitive performance with higher efficiency.

3. Methodology

Overview of AStar This section introduces AStar in detail. As shown in Figure 3 and Algorithm 1, our approach consists of three steps:

- *Visual Reasoning Action Definition:* Establish six human-like reasoning actions as building blocks for chain-structured thought cards.
- *MCTS-Powered Thought Card Construction:* Leverage MCTS to systematically construct thought cards, which serve as reference insights during inference.
- *Adaptive Reasoning and Verification:* Dynamically select and execute optimal reasoning patterns based on problem complexity, followed by solution verification.

3.1. Visual Reasoning Action Definition

Understanding human complex reasoning is crucial for modeling cognitive processes (Jaffe et al., 2023). Existing studies distinguish between two cognitive systems: System 1

and System 2 (Kahneman, 2011; Da Silva, 2023). While “System 1” represents fast, intuitive, yet error-prone thinking, “System 2” involves slow, deliberative thinking with superior performance. With the emergence of advanced models like OpenAI o1 (OpenAI, 2024) and QVQ (Team, 2024), developing efficient “System 2” approaches to emulate human cognitive processes has gained significant research attention (Xu et al., 2024; Yao et al., 2024; Thawakar et al., 2025). Inspired by this, we introduce six vision-language reasoning actions to bridge the gap between model reasoning and human cognition: *Visual Parsing* (VP, a_1), *System Analysis* (SA, a_2), *One-Step Thought* (OST, a_3), *Chain-of-Thought* (CoT, a_4), *Divide and Conquer* (DC, a_5), *Self-Reflection* (SR, a_6). Details are provided in Appendix B.1.

3.2. MCTS-Powered Thought Card Construction

Following the action definition, we introduce “*thought cards*” as structured reasoning templates to guide inference in Sec. 3.3. Using a small seed dataset, we first derive reasoning paths (Phase 1) and then distill them into high-level thought cards (Phase 2). These cards serve as prior insights during inference, providing structured guidance for efficient problem-adaptive reasoning.

Phase 1: Acquire reasoning paths for seed data As shown in Figure 3, we employ MCTS to iteratively optimize the solution search process, generating high-quality reasoning paths for the seed dataset. This design leverages MCTS’s systematic exploration (Ye et al., 2021) and MLLMs’ inherent reasoning capabilities (Yin et al., 2023; Wang et al., 2024f). We formulate each multimodal reasoning problem x (consisting of input question and images) as a tree search problem, where x represents the root node and subsequent nodes denote reasoning steps (actions and corresponding outcomes) generated by a policy MLLM π_θ . We define the state S_{t-1} as the trajectory x, s_1, \dots, s_{t-1} , where $S_0 = x$. The next step is sampled as $s_t \sim \pi_\theta(S_{t-1})$. To guide tree expansion, we define $Q(s)$ as the reward value for node s . Initially, all unexplored nodes are assigned $Q(s_i) = 0$. They are updated using a weighted average between the parent’s current value and its child node’s value:

$$Q(p) \leftarrow (1 - \alpha)Q(p) + \alpha Q(s) \quad (1)$$

where α is a discount factor for future rewards. For terminal nodes, following Zhou et al. (2024); Wu et al. (2024a), we adopt the likelihood of self-consistency majority voting as the reward value, enabling supervision-free generalization.

Specifically, this phase comprises four MCTS operations:

(1) *Selection*. This operation identifies promising nodes for expansion. Starting from the root node, we iteratively select child nodes using the Upper Confidence Bounds applied to Trees (UCT) (Kocsis & Szepesvári, 2006) until reaching a

Algorithm 1 Multimodal Reasoning with AStar

Input: a policy model π_θ ; a multimodal test question x_t ; a set of seed data D_s
// 3.1. Visual Reasoning Action Definition
Initialize action space $A = \{a_1, a_2, a_3, a_4, a_5, a_6\}$
// 3.2. MCTS-Powered Thought Card Construction
 $D \leftarrow []$; $Cards \leftarrow \{\}$
for $(x, y) \in D_s$ **do**
 $\{x, y, P\} \leftarrow \text{MCTS}(\pi_\theta; x)$
 if found an valid reasoning path then
 Find p_{best} from P
 Add $\{x, p_{\text{best}}\}$ into D
 Update $Cards$ from D
 end if
end for
// 3.3. Adaptive Reasoning and Verification
 $c \leftarrow \text{CardMatch}(Cards; x_t)$
 $y_t \leftarrow \text{ReasonAndVerify}(\pi_\theta; x_t; c)$
Output: the optimal reasoning trajectory y_t

leaf node:

$$UCT(s) = Q(s) + w \sqrt{\frac{\ln N(p)}{N(s)}} \quad (2)$$

where $Q(s)$ is the reward value for node s , $N(s)$ is the visit count, p is the parent node, and w is the exploration weight. The node with the highest UCT value is selected for subsequent phases, balancing exploration and exploitation.

(2) *Expansion*. The selected node s is expanded by sampling n actions from π_θ and generating corresponding reasoning outcomes. These n child nodes are added to the tree and stored in an external memory structure.

(3) *Simulation*. Starting from the selected node, we iteratively sample and expand nodes until reaching a terminal state (maximum depth or answer node).

(4) *Backpropagation*. Upon simulation completion, node information is updated along the simulation path s_0, \dots, s_d . Visit counts are incremented ($N(s) \leftarrow N(s) + 1$), and node value $Q(s)$ is propagated backward to its parent node p using Equation 1. These updated values are used to guide subsequent UCT-based node selection.

Phase 2: Distill paths into thought cards After executing MCTS, we obtain a tree structure for each seed dataset question, yielding multiple valid reasoning paths that constitute the path set P . Inspired by the concept of Value of Computation (VOC) (Russell & Wefald, 1991), which optimizes the trade-off between computational benefits and costs, we propose a VOC-inspired selection metric to identify the optimal reasoning trajectory from candidate solutions:

$$\text{Score}(x, p_x) = k \cdot R(p_x|x) - (1 - k) \cdot C(p_x) \quad (3)$$

where x is the task input, p_x represents a candidate reasoning path from P , and k balances computational benefits against costs. Here, for simplicity, $R(p_x|x)$ denotes the path’s final reward (defined as the leaf node’s Q-value), while $C(p_x)$ measures the reasoning cost (defined as the number of actions in the sequence).

Then, for each question in seed dataset, we select path p_{best} with highest $Score(x, p_x)$ to build a *Question-path repository* D with one-to-one mappings. Inspired by metareasoning principles (Russell & Wefald, 1991; Roberts & Roberts, 2024), which advocate for adaptive reasoning strategies, we distill these question-path pairs into abstract thought cards \mathbb{C} using Problem Condition Complexity (PCC) (Lee & Heyworth, 2000; Embretson & Daniel, 2008), a cognitive complexity metric designed for complex reasoning. Each card represents a high-level reasoning pattern abstracted from multiple prior problems, enabling efficient transfer of reasoning insights during inference in the next step.

3.3. Adaptive Reasoning and Verification

During inference, given a multimodal test query x_t , we compute its PCC and perform nearest neighbor matching (Muja & Lowe, 2014) against pre-constructed thought cards \mathbb{C} to identify the most relevant five cards that best align with its complexity level. The selection process is formalized as:

$$NN_5(x_t, \mathbb{C}) = \arg \min_{\mathbb{C}_{x_t} \subseteq \mathbb{C}, |\mathbb{C}_{x_t}|=5} \sum_{c \in \mathbb{C}_{x_t}} d(x_t, c) \quad (4)$$

where $NN_5(x_t, \mathbb{C}) \subseteq \mathbb{C}$ is the closest subset to x_t , determined by the distance $d: \mathbb{R} \times \mathbb{R} \rightarrow \mathbb{R}$. By leveraging these reasoning templates, our method maintains the benefits of tree-structured reasoning without extensive node expansion, enabling efficient generation of candidate solutions.

Identifying the optimal reasoning trajectory among these candidates represents a critical challenge (Luo et al., 2025). Given the scarcity of verification models in the visual domain, we employ both self-consistency checks and text-domain outcome reward models to select the final solution.

In summary, our approach can be viewed as an optimized variant of tree search algorithms. Unlike traditional MCTS methods that require extensive exploration, we strategically reduce computational complexity by incorporating prior insights through thought cards. As shown in Figure 3, this enables efficient tree traversal along promising trajectories while maintaining high performance, offering valuable insights for developing efficient reasoning strategies.

4. Experiments

The section presents 4.1 experimental setup and assesses AStar’s effectiveness from four aspects: 4.2 performance, 4.3 data and computational efficiency, 4.4 out-of-distribution

generalization, and 4.5 ablation study and analysis.

4.1. Experimental Setup

Datasets We perform extensive experiments across three reasoning tasks and six datasets: (1) general visual question answering: ChartQA (Masry et al., 2022) and MMStar (Chen et al., 2024b); (2) mathematical reasoning: MathVista (Lu et al., 2023), MathVerse (Zhang et al., 2025), and MathVision (Wang et al., 2024a); (3) commonsense and scientific reasoning: GAOKAO-MM (Zong & Qiu, 2024).

Models To demonstrate the versatility of AStar, we evaluate its effectiveness on both LLM and MLLM, including Qwen2.5-7B (Qwen Team, 2024), Qwen2-VL-2B (Wang et al., 2024b), and Qwen2-VL-7B. This design aims to validate that AStar can seamlessly leverage pre-trained LLM and MLLM as its inference backbone without modifications.

Baselines We evaluate AStar against four strong baseline categories: (1) open-source general MLLMs, including the powerful Qwen2-VL (Wang et al., 2024b) and InternVL2 series (Chen et al., 2024d); (2) open-source MLLMs specifically optimized for mathematical reasoning, such as recent work URSA (Luo et al., 2025) and Math-LLaVA (Shi et al., 2024); (3) advanced closed-source MLLMs, including GPT-4V (OpenAI, 2023), and GPT-4o (OpenAI, 2024); and (4) tree-based methods, such as AR-MCTS (Dong et al., 2024a) and Mulberry (Yao et al., 2024).

4.2. Performance Comparison with Baselines

Results on Diverse Reasoning Benchmarks Table 1 and 2 presents the performance of AStar across four mainstream reasoning benchmarks. We have four key findings:

◇ AStar consistently outperforms both powerful open-source general and math-specialized MLLMs across general visual question answering and mathematical reasoning tasks. Specifically, using Qwen2.5-7B as the reasoning backbone, our method achieves 54.0% accuracy on MathVerse, surpassing InternVL2-8B by 18.1% and the recent high-quality CoT-enhanced URSA-7B model by 8.3%.

◇ AStar demonstrates strong performance across multiple reasoning capabilities. Notably, it achieves 63.1% accuracy on logical reasoning (LOG), outperforming InternVL2-8B by 50.5% and URSA-7B by 39.7%. Similar improvements are observed in statistical reasoning (STA: 68.8%) and visual question answering (VQA: 60.1%).

◇ The benefits of AStar’s adaptive reasoning are universal and maintain consistent performance improvements across varying degrees of multimodal information content. Notably, our method achieves consistent gains across different information distributions, from vision-intensive (VI: 46.8%) and vision-dominant (VD: 61.8%) to text-dominant (TD:

Table 1. Evaluation of AStar’s reasoning capabilities on MathVista and MathVerse *testmini*. The best results are highlighted in **bold**. For MathVista, we pick five categories: ALL (overall accuracy), ARI (arithmetic reasoning), LOG (logical reasoning), STA (statistical reasoning), and VQA (visual question answering). For MathVerse, we present seven categories: ALL (overall accuracy), VI (vision intensive), VD (vision dominant), VO (vision only), TD (text dominant), TL (text lite), and TO (text only).

Model	#Params	MathVista					MathVerse						
		ALL	ARI	LOG	STA	VQA	ALL	VI	VD	VO	TD	TL	TO
Random	-	17.9	13.8	13.4	14.3	26.3	12.4	12.4	12.4	12.4	12.4	12.4	12.4
Human	-	60.3	59.2	40.7	63.9	55.9	64.9	61.4	68.3	66.7	71.2	70.9	41.7
<i>Open-Source General MLLMs</i>													
mPLUG-Owl2-7B (Ye et al., 2023)	7B	22.2	19.2	13.5	21.4	27.9	10.3	11.1	9.4	8.0	11.6	11.4	13.8
MiniGPT4-7B (Zhu et al., 2023)	7B	23.1	32.0	10.8	17.9	30.2	12.2	12.5	14.8	8.7	12.3	12.9	13.4
LLaVA-1.5-13B (Liu et al., 2024a)	13B	27.7	28.6	10.8	22.9	30.2	12.7	12.6	12.7	9.0	17.1	12.0	22.6
SPHINX-V2-13B (Lin et al., 2023)	13B	36.7	33.4	24.3	51.5	43.0	16.1	16.4	15.6	16.2	20.8	14.1	14.0
SPHINX-MoE (Lin et al., 2023)	8×7B	42.6	43.0	14.4	50.8	43.3	22.8	21.1	19.6	18.3	33.3	21.9	23.1
LLaVA-NeXT-34B (Liu et al., 2024b)	34B	46.5	-	-	-	-	34.6	35.2	28.9	22.4	49.0	37.6	30.1
InternLM-XComposer2-VL (Dong et al., 2024c)	7B	57.6	51.6	13.5	62.8	39.7	25.9	20.1	24.4	19.8	36.9	28.3	42.5
Deepseek-VL (Lu et al., 2024)	7B	34.9	38.8	18.9	33.2	34.6	19.3	20.2	18.4	11.8	23.0	23.2	23.1
InternVL2-8B (Chen et al., 2024d)	8B	58.3	56.4	10.8	68.8	49.7	35.9	32.2	30.9	27.7	39.0	33.8	36.0
Qwen2-VL (Wang et al., 2024b)	7B	58.9	57.5	24.3	43.1	58.1	33.6	31.3	30.3	28.1	37.4	33.5	35.0
<i>Open-Source Math MLLMs (Large-Scale Training)</i>													
G-LLaVA-7B (Gao et al., 2023)	7B	25.1	19.4	15.2	15.1	28.7	16.6	17.2	14.6	9.4	20.9	20.7	21.1
Math-LLaVA-13B (Shi et al., 2024)	13B	46.6	40.7	23.3	42.3	33.5	22.9	24.5	21.7	16.1	27.3	24.9	27.0
Math-PUMA-Qwen2-7B (Zhuang et al., 2024)	7B	47.9	46.2	21.6	55.8	30.2	33.6	33.4	31.6	26.0	42.1	35.0	39.8
Math-PUMA-DeepSeek-Math (Zhuang et al., 2024)	7B	44.7	41.9	8.1	50.8	31.3	31.8	33.6	31.6	14.7	43.4	35.4	47.5
MAVIS-7B (Zhang et al., 2024d)	7B	-	-	-	-	-	35.2	34.1	29.7	31.8	43.2	37.2	-
InfMM-Math (Han et al., 2024)	7B	-	-	-	-	-	34.5	38.1	32.4	15.8	46.7	32.4	-
MultiMath-7B (Peng et al., 2024)	7B	50.0	42.2	23.3	64.9	49.2	27.7	28.1	25.9	15.0	34.8	30.8	35.3
URSA-7B (Luo et al., 2025)	7B	59.8	53.5	21.6	57.1	40.2	45.7	46.4	43.9	28.6	55.3	48.3	51.8
AStar (Ours, Training-free Reasoning)	7B	63.5	63.1	61.3	68.8	60.1	54.0	46.8	61.8	46.4	53.9	44.3	53.9

Table 2. Comparison with powerful baselines on general VQA datasets: MMStar and ChartQA.

Model	#Params	MMStar	ChartQA
<i>2B-Scale Baselines</i>			
Qwen2-VL (Wang et al., 2024b)	2B	48.0	73.5
Mulberry (Yao et al., 2024)	2B	51.3	77.7
AStar (Ours)	2B	51.7	78.3
<i>≥ 7B-Scale Baselines</i>			
Deepseek-VL (Lu et al., 2024)	7B	36.1	59.1
Qwen2-VL (Wang et al., 2024b)	7B	60.7	83.0
InternVL2 (Chen et al., 2024d)	8B	61.5	83.3
Insight-V (Dong et al., 2024d)	7B	61.5	82.3
Mulberry (Yao et al., 2024)	7B	61.3	83.9
LLaVA-CoT (Xu et al., 2024)	11B	58.1	-
LlamaV-o1 (Thawakar et al., 2025)	11B	59.5	-
AStar (Ours)	7B	61.7	83.9

53.9%) and text-only (TO: 53.9%) scenarios, demonstrating robust performance regardless of the modality balance.

◇ Beyond specialized reasoning tasks, AStar performs superior on general VQA benchmarks (MMStar and ChartQA), suggesting that enhanced reasoning capabilities also benefit general visual understanding.

Results on More Challenging Datasets As shown in Figure 4, we evaluate AStar against leading models on the chal-

lenging MathVision benchmark (Wang et al., 2024a) across multiple reasoning dimensions. AStar achieves 32.3% average accuracy across all dimensions, surpassing GPT-4o (30.4%). Notably, in logical reasoning area, AStar attains 45.8% accuracy, outperforming both GPT-4o (29.4%) and Math-LLaVA-13B (16.0%). AStar’s effectiveness can be attributed to its adaptive tree-structured decomposition framework, which simplifies complex multimodal reasoning tasks into manageable sub-problems, enabling substantial improvements across diverse reasoning capabilities.

Comparison with Leading MLLMs We further compare AStar against leading closed-source and larger open-source models. As illustrated in Figure 5, AStar-empowered models deliver competitive performance, matching or surpassing larger models. Notably, AStar-7B achieves an average score of 50.0% across three challenging benchmarks, outperforming GPT-4o (48.1%) and Qwen2-VL-72B (46.0%). Additionally, our reasoning paradigm enables Qwen2-VL-2B to surpass the larger Qwen2-VL-7B model.

4.3. Data and Computational Efficiency

We further compare our approach AStar with two recent powerful multimodal tree search methods: AR-MCTS (Dong et al., 2024a) and Mulberry (Yao et al., 2024). As shown in Table 3, we compare multiple dimensions, includ-

Table 3. Comparison with leading multimodal tree search methods. AStar achieves competitive performance with only 0.5K prior data and 5 search iterations per sample, demonstrating superior efficiency and effectiveness.

Methods	Open-Source Only	Training-Free	Data Volume	Search Iter. ↓	MathVista Acc. ↑	MMStar Acc. ↑	GAOKAO Acc. ↑
AR-MCTS (Dong et al., 2024a)	✓	✗	34.5K	32.0	64.1	-	37.4
Mulberry (Yao et al., 2024)	✗	✗	260K	-	63.1	61.3	-
Ours	✓	✓	0.5K	5.0	63.5	61.7^{0.4}†	49.7^{12.3}†

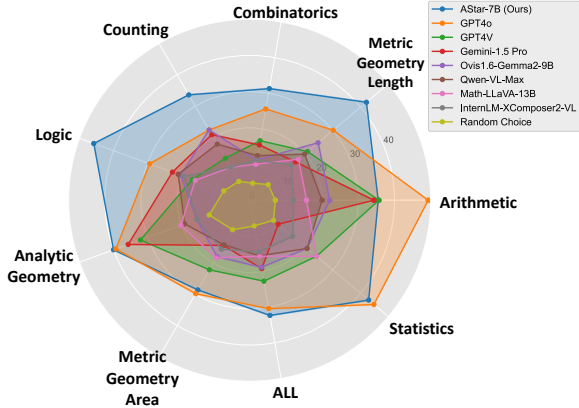


Figure 4. Comparison with leading MLLMs across various capabilities on the challenging MathVision dataset. Our 7B-parameter model achieves comparable performance to GPT-4o.

ing training requirements, training data volume, computational efficiency (measured by average search iterations per sample), and accuracy on three representative benchmarks.

Results demonstrate that AStar achieves competitive performance while significantly improving both data and computational efficiency. In terms of data efficiency, AStar requires only 0.5K prior samples, which represents a 69-fold reduction compared to AR-MCTS (34.5K) and a 520-fold reduction compared to Mulberry (260K), respectively. This efficiency stems from explicit reasoning pattern extraction, enabling performance comparable to implicit learning methods with far less training data. Such efficiency is particularly advantageous in limited-data scenarios. Regarding computational efficiency, AStar reduces the average iterations per sample by 6.4× compared to AR-MCTS, while maintaining comparable or superior accuracy across all benchmarks.

4.4. Out-of-Distribution Generalization

Recent work has highlighted that distributional shifts severely affect the reliability of MLLMs (Yin et al., 2023; Zhang et al., 2024f). While these models excel in in-distribution (ID) tasks, their performance often degrades in out-of-distribution (OOD) scenarios (Dong et al., 2024b; Miyai et al., 2024), a challenge further compounded by the difficulty of acquiring sufficient high-quality training data.

In this section, we evaluate AStar’s performance in OOD

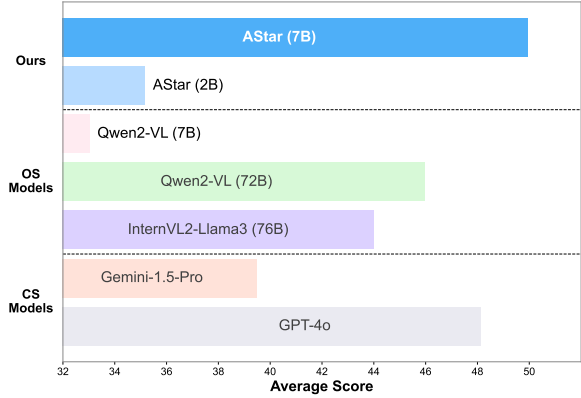


Figure 5. Comparison between AStar and powerful MLLMs across 3 challenging benchmarks: MathVista, MathVerse, and MathVision. ‘OS’ and ‘CS’ denote open-source and closed-source models. AStar with 7B model outperforms larger OS and CS models.

scenarios. Since our reasoning guidance during inference is derived from the mathematical domain, we further test on GAOKAO-MM (Zong & Qiu, 2024), a Chinese human-level multimodal reasoning benchmark that includes historical, geographical, and scientific reasoning tasks. This design naturally constitutes an OOD evaluation setting. As shown in Figure 6, all models demonstrate significant improvements over baseline methods when enhanced with the AStar framework. Notably, for Qwen2-VL-7B, our method improves Geography task accuracy from 26.9% to 51.6% and achieves an average improvement of 19.5% across all subjects. These results validate AStar’s strong generalization across different languages, task distributions, and reasoning domains, establishing it as a robust and versatile approach for both ID and OOD reasoning tasks.

4.5. Ablation Study and Analysis

To investigate the contribution of each component in AStar, we conduct ablation study as shown in Table 4. Here, “w/o” denotes variants with specific components removed. Our analysis reveals three key findings:

First, removing any component leads to performance degradation, validating the necessity of all component designs. Specifically, excluding the card construction module results in the most substantial drops (4.6% on MathVista and 5.5% on MathVerse), highlighting the critical role of thought cards

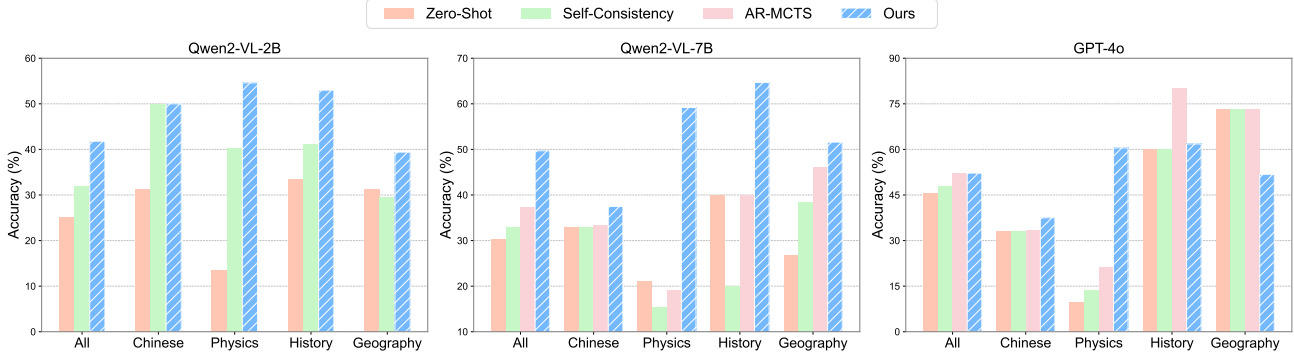


Figure 6. Cross-distribution performance comparison on GAOKAO-MM. We test on Qwen2-VL-2B, Qwen2-VL-7B, and GPT-4o. Results highlight that AStar exhibits superior performance when testing on out-of-distribution data.

Table 4. Ablation results on AStar-7B. ‘RA’, ‘RC’, ‘RS’, ‘SC’ denotes ‘random actions’, ‘random card’, ‘random selection’, and ‘self-consistency’, respectively. We observe that every component is important for optimal performance.

Model Setting	MathVista	MathVerse	Average
AStar	63.5	54.0	58.8
– w/o thought cards (RA)	58.9	48.5	53.7 ^{-5.1↓}
– w/o card match (RC)	61.3	50.3	55.8 ^{-3.0↓}
– w/o verification (RS)	62.0	51.6	56.8 ^{-2.0↓}
– w/o verification (SC)	63.0	51.8	57.4 ^{-1.4↓}

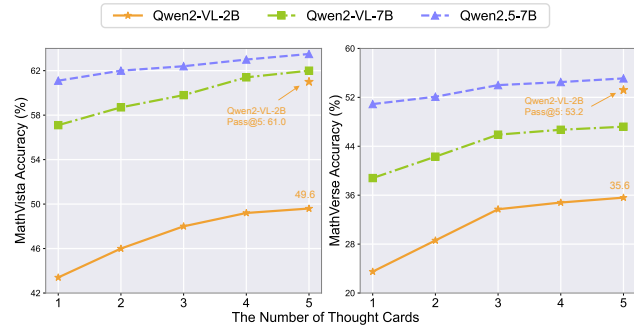


Figure 7. Inference Time Scaling. We examine the variation in AStar performance with the number of selected reasoning guidance-providing thought cards in Sec. 3.3.

in providing high-level insights for test-time inference.

Second, the precision of card matching also impacts performance, particularly on complex tasks like MathVerse where degradation is more pronounced than on MathVista. While this paper employs PCC-based nearest-neighbor matching, future work could explore more advanced strategies.

Third, while the verification module improves performance, simpler alternatives like self-consistency (SC) or random selection (RS) show only modest degradation (2.0% and 1.4%). This resilience suggests that thought card guidance enables robust candidate solution generation even with basic selection methods.

Inference Time Scaling We gradually increase the number of selected thought cards during inference to investigate whether our method follows test-time scaling laws. Figure 7 demonstrates that incorporating additional reasoning guidance via thought cards leads to consistent performance improvements in our AStar framework.

Visualization of Sampling Space To analyze the diversity of solutions generated by our AStar-powered reasoning framework across varying numbers of thought cards, we conduct a visualization study here. We sample 250 problems from MathVision and generate 2 candidate solutions for each problem using AStar (Qwen2-VL-2B), resulting

in 500 total samples. Following Dong et al. (2024a), we employ a three-step analysis process using BGE-M3 (Chen et al., 2024a) for semantic embedding, followed by dimensionality reduction (PCA) and clustering techniques, DBSCAN (Ester et al., 1996).

Figure 8 and 9 illustrate the visualization results across varying numbers of thought cards ($k = 2$ and $k = 5$) on MathVista and MathVision, respectively. The empirical analysis reveals consistent conclusions across both standard mathematical reasoning tasks (MathVista) and challenging scenarios (MathVision). When fewer thought cards are provided ($k = 2$), the model generates clusters with fewer centroids for the same problem set, indicating a more constrained sampling space with limited potential. Conversely, increasing the number of thought cards to $k = 5$ leads to clusters with more centroids, suggesting a richer sampling space with higher performance potential. The modest difference in cluster counts between $k = 2$ and $k = 5$ indicates that our framework effectively adapts to problem complexity by dynamically selecting suitable reasoning patterns from high-quality thought cards. Even with fewer thought cards, it maintains robust sampling diversity and performance through this adaptive matching mechanism.

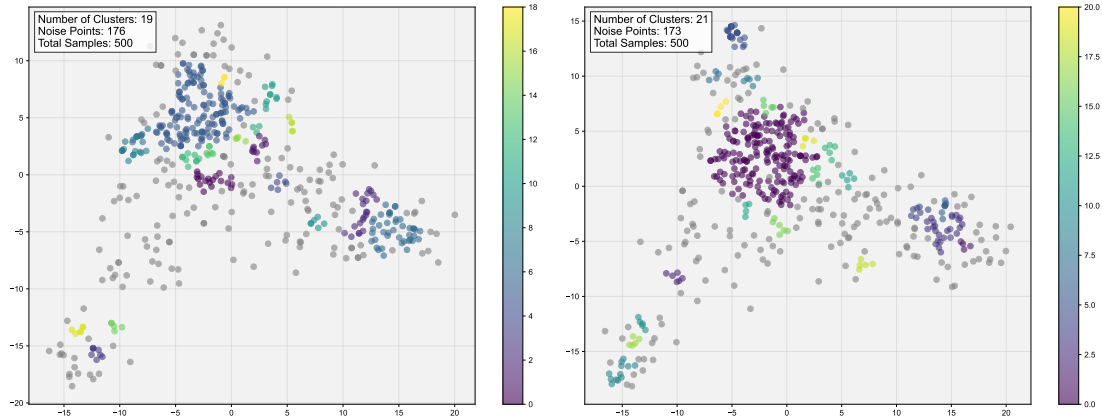


Figure 8. Visualization of candidate reasoning paths on MathVista with $k = 2$ (left) and $k = 5$ (right) thought cards. Dots represent individual reasoning steps, while colors indicate distinct solution clusters. The increasing density and diversity of clusters from left to right demonstrate the model’s enhanced exploration capability with more thought cards, leading to more comprehensive coverage of the solution space.

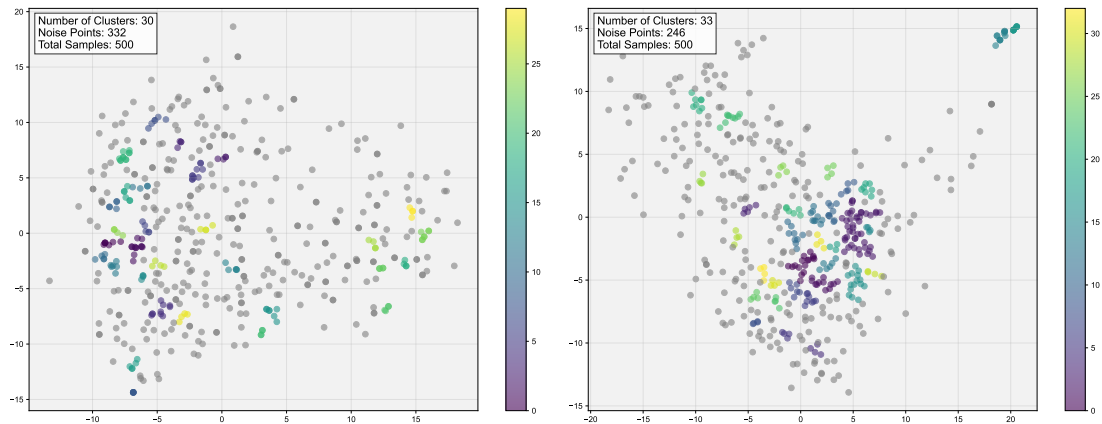


Figure 9. Visualization of candidate reasoning paths on MathVision with $k = 2$ (left) and $k = 5$ (right) thought cards. Dots represent individual reasoning steps, while colors indicate distinct solution clusters. The increasing density and diversity of clusters from left to right demonstrate the model’s enhanced exploration capability with more thought cards, leading to more comprehensive coverage of the solution space.

Notably, the observed lower cluster count in MathVista compared to MathVision offers valuable insights into task-specific reasoning requirements. On MathVista, which contains relatively simpler problems, our AStar framework exhibits strong reasoning path convergence: multiple high-quality thought cards typically lead to consistent solutions. This convergence allows for effective performance even with basic self-consistency verification. However, on the more challenging MathVision dataset, we observe greater path divergence, emphasizing the importance of careful validation and selection of optimal reasoning paths. This behavior closely resembles human problem-solving patterns. When addressing elementary problems, different approaches tend to naturally converge to the same answer. In contrast,

for complex challenges like Olympic problems, diverse approaches often yield different conclusions, making thorough solution validation necessary.

In summary, our visualization results empirically validate that AStar effectively addresses the challenge of limited diversity in candidate solutions, enabling comprehensive coverage of the problem-solving space while providing robust prior guidance for efficient inference.

5. Conclusion

In this paper, we propose AStar, a novel automated structured thinking paradigm for multimodal reasoning that ef-

fectively tackles both performance and efficiency challenges in visual reasoning tasks. By leveraging the hierarchical structure of MCTS and extracting high-level cognitive reasoning patterns to guide inference, our approach achieves notable advantages: (1) 32.3% accuracy on the challenging MathVision benchmark with a 7B backbone, surpassing GPT-4o’s 30.4%; (2) $6.4\times$ reduction in inference overhead compared to existing tree-based methods; and (3) $520\times$ less prior data than training-based approaches while maintaining comparable performance. These results demonstrate that AStar’s integration of structured decomposition with efficient prior guidance offers a promising pathway for advancing multimodal reasoning, making it both more powerful and accessible to the broader research community.

References

- Anthropic. Introducing the next generation of claude, March 2024. URL <https://www.anthropic.com/news/claude-3-family>.
- Bai, J., Bai, S., Yang, S., Wang, S., Tan, S., Wang, P., Lin, J., Zhou, C., and Zhou, J. Qwen-vl: A versatile vision-language model for understanding, localization, text reading, and beyond. *arXiv preprint arXiv:2308.12966*, 1(2): 3, 2023.
- Bansal, H., Hosseini, A., Agarwal, R., Tran, V. Q., and Kazemi, M. Smaller, weaker, yet better: Training llm reasoners via compute-optimal sampling. *arXiv preprint arXiv:2408.16737*, 2024.
- Chaslot, G., Bakkes, S., Szita, I., and Spronck, P. Monte-carlo tree search: A new framework for game ai. In *Proceedings of the AAAI Conference on Artificial Intelligence and Interactive Digital Entertainment*, volume 4, pp. 216–217, 2008.
- Chen, J., Li, D. Z. X. S. X., Zhang, Z. L. P., Xiong, R. K. V. C. Y., and Elhoseiny, M. Minigt-v2: Large language model as a unified interface for vision-language multi-task learning. *arXiv preprint arXiv:2310.09478*, 2023.
- Chen, J., Xiao, S., Zhang, P., Luo, K., Lian, D., and Liu, Z. BGE m3-embedding: Multi-lingual, multi-functionality, multi-granularity text embeddings through self-knowledge distillation. *CoRR*, abs/2402.03216, 2024a.
- Chen, L., Li, J., Dong, X., Zhang, P., Zang, Y., Chen, Z., Duan, H., Wang, J., Qiao, Y., Lin, D., and Zhao, F. Are we on the right way for evaluating large vision-language models? In *The Thirty-eighth Annual Conference on Neural Information Processing Systems*, 2024b.
- Chen, Z., Wang, W., Cao, Y., Liu, Y., Gao, Z., Cui, E., Zhu, J., Ye, S., Tian, H., Liu, Z., et al. Expanding performance boundaries of open-source multimodal models with model, data, and test-time scaling. *arXiv preprint arXiv:2412.05271*, 2024c.
- Chen, Z., Wu, J., Wang, W., Su, W., Chen, G., Xing, S., Zhong, M., Zhang, Q., Zhu, X., Lu, L., et al. Internvl: Scaling up vision foundation models and aligning for generic visual-linguistic tasks. In *Proceedings of the IEEE/CVF Conference on Computer Vision and Pattern Recognition*, pp. 24185–24198, 2024d.
- Cobbe, K., Kosaraju, V., Bavarian, M., Chen, M., Jun, H., Kaiser, L., Plappert, M., Tworek, J., Hilton, J., Nakano, R., et al. Training verifiers to solve math word problems. *arXiv preprint arXiv:2110.14168*, 2021.
- Cui, C., Ma, Y., Cao, X., Ye, W., Zhou, Y., Liang, K., Chen, J., Lu, J., Yang, Z., Liao, K.-D., et al. A survey on multimodal large language models for autonomous driving. In *Proceedings of the IEEE/CVF Winter Conference on Applications of Computer Vision*, pp. 958–979, 2024.
- Da Silva, S. System 1 vs. system 2 thinking. *Psych*, 5(4): 1057–1076, 2023.
- Dong, G., Zhang, C., Deng, M., Zhu, Y., Dou, Z., and Wen, J.-R. Progressive multimodal reasoning via active retrieval. *arXiv preprint arXiv:2412.14835*, 2024a.
- Dong, H., Ding, Z., and Zhang, S. *Deep Reinforcement Learning: Fundamentals, Research and Applications*, volume 1 of *eBook Packages: Mathematics and Statistics*. Springer Singapore, 1 edition, 2020. ISBN 9789811540950.
- Dong, H., Zhao, Y., Chatzi, E., and Fink, O. MultiOOD: Scaling out-of-distribution detection for multiple modalities. In *The Thirty-eighth Annual Conference on Neural Information Processing Systems*, 2024b.
- Dong, X., Zhang, P., Zang, Y., Cao, Y., Wang, B., Ouyang, L., Wei, X., Zhang, S., Duan, H., Cao, M., et al. Internlm-xcomposer2: Mastering free-form text-image composition and comprehension in vision-language large model. *arXiv preprint arXiv:2401.16420*, 2024c.
- Dong, Y., Liu, Z., Sun, H.-L., Yang, J., Hu, W., Rao, Y., and Liu, Z. Insight-v: Exploring long-chain visual reasoning with multimodal large language models. *arXiv preprint arXiv:2411.14432*, 2024d.
- Driess, D., Xia, F., Sajjadi, M. S., Lynch, C., Chowdhery, A., Ichter, B., Wahid, A., Tompson, J., Vuong, Q., Yu, T., et al. Palm-e: An embodied multimodal language model. *arXiv preprint arXiv:2303.03378*, 2023.
- Du, Y., Liu, Z., Li, Y., Zhao, W. X., Huo, Y., Wang, B., Chen, W., Liu, Z., Wang, Z., and Wen, J.-R. Virgo:

- A preliminary exploration on reproducing o1-like mllm. *arXiv preprint arXiv:2501.01904*, 2025.
- Embretson, S. E. and Daniel, R. C. Understanding and quantifying cognitive complexity level in mathematical problem solving items. *Psychology Science*, 50(3):328, 2008.
- Ester, M., Kriegel, H., Sander, J., and Xu, X. A density-based algorithm for discovering clusters in large spatial databases with noise. In Simoudis, E., Han, J., and Fayyad, U. M. (eds.), *Proceedings of the Second International Conference on Knowledge Discovery and Data Mining (KDD-96)*, Portland, Oregon, USA, pp. 226–231. AAAI Press, 1996.
- Gao, B., Cai, Z., Xu, R., Wang, P., Zheng, C., Lin, R., Lu, K., Lin, J., Zhou, C., Xiao, W., et al. Llm critics help catch bugs in mathematics: Towards a better mathematical verifier with natural language feedback. *CoRR*, 2024.
- Gao, J., Pi, R., Zhang, J., Ye, J., Zhong, W., Wang, Y., Hong, L., Han, J., Xu, H., Li, Z., et al. G-llava: Solving geometric problem with multi-modal large language model. *arXiv preprint arXiv:2312.11370*, 2023.
- Ge, Z., Huang, H., Zhou, M., Li, J., Wang, G., Tang, S., and Zhuang, Y. Worldgpt: Empowering llm as multi-modal world model. In *Proceedings of the 32nd ACM International Conference on Multimedia*, pp. 7346–7355, 2024.
- Goertzel, B. and Pennachin, C. *Artificial general intelligence*, volume 2. Springer, 2007.
- Han, X., Jian, Y., Hu, X., Liu, H., Wang, Y., Fan, Q., Ai, Y., Huang, H., He, R., Yang, Z., et al. Infimm-webmath-40b: Advancing multimodal pre-training for enhanced mathematical reasoning. In *The 4th Workshop on Mathematical Reasoning and AI at NeurIPS'24*, 2024.
- Hao, S., Gu, Y., Ma, H., Hong, J., Wang, Z., Wang, D., and Hu, Z. Reasoning with language model is planning with world model. In Bouamor, H., Pino, J., and Bali, K. (eds.), *Proceedings of the 2023 Conference on Empirical Methods in Natural Language Processing*, pp. 8154–8173, Singapore, December 2023. Association for Computational Linguistics.
- Hartsock, I. and Rasool, G. Vision-language models for medical report generation and visual question answering: A review. *Frontiers in Artificial Intelligence*, 7:1430984, 2024.
- Hu, Y., Shi, W., Fu, X., Roth, D., Ostendorf, M., Zettlemoyer, L., Smith, N. A., and Krishna, R. Visual sketchpad: Sketching as a visual chain of thought for multimodal language models. *arXiv preprint arXiv:2406.09403*, 2024.
- Jaffe, P. I., Poldrack, R. A., Schafer, R. J., and et al. Modelling human behaviour in cognitive tasks with latent dynamical systems. *Nature Human Behaviour*, 7:986–1000, 2023.
- Kahneman, D. *Thinking, Fast and Slow*. Farrar, Straus and Giroux, New York, NY, 2011. ISBN 978-0374275631.
- Kocsis, L. and Szepesvári, C. Bandit based monte-carlo planning. In Fürnkranz, J., Scheffer, T., and Spiliopoulou, M. (eds.), *Machine Learning: ECML 2006*, pp. 282–293, Berlin, Heidelberg, 2006. Springer Berlin Heidelberg. ISBN 978-3-540-46056-5.
- Langley, P. Crafting papers on machine learning. In Langley, P. (ed.), *Proceedings of the 17th International Conference on Machine Learning (ICML 2000)*, pp. 1207–1216, Stanford, CA, 2000. Morgan Kaufmann.
- Lee, F.-L. and Heyworth, R. Problem complexity: A measure of problem difficulty in algebra by using computer. *Education Journal*, 28(1):85–108, 2000.
- Li, B., Zhang, Y., Guo, D., Zhang, R., Li, F., Zhang, H., Zhang, K., Zhang, P., Li, Y., Liu, Z., et al. Llava-onevision: Easy visual task transfer. *arXiv preprint arXiv:2408.03326*, 2024.
- Li, Y., Lin, Z., Zhang, S., Fu, Q., Chen, B., Lou, J.-G., and Chen, W. Making language models better reasoners with step-aware verifier. In Rogers, A., Boyd-Graber, J., and Okazaki, N. (eds.), *Proceedings of the 61st Annual Meeting of the Association for Computational Linguistics (Volume 1: Long Papers)*, pp. 5315–5333, Toronto, Canada, July 2023. Association for Computational Linguistics.
- Lightman, H., Kosaraju, V., Burda, Y., Edwards, H., Baker, B., Lee, T., Leike, J., Schulman, J., Sutskever, I., and Cobbe, K. Let’s verify step by step. In *The Twelfth International Conference on Learning Representations*, 2024.
- Lin, Z., Liu, C., Zhang, R., Gao, P., Qiu, L., Xiao, H., Qiu, H., Lin, C., Shao, W., Chen, K., et al. Sphinx: The joint mixing of weights, tasks, and visual embeddings for multi-modal large language models. *arXiv preprint arXiv:2311.07575*, 2023.
- Liu, H., Li, C., Li, Y., and Lee, Y. J. Improved baselines with visual instruction tuning. In *Proceedings of the IEEE/CVF Conference on Computer Vision and Pattern Recognition*, pp. 26296–26306, 2024a.
- Liu, H., Li, C., Li, Y., Li, B., Zhang, Y., Shen, S., and Lee, Y. J. Llava-next: Improved reasoning, ocr, and world knowledge, 2024b.

- Lu, H., Liu, W., Zhang, B., Wang, B., Dong, K., Liu, B., Sun, J., Ren, T., Li, Z., Yang, H., et al. Deepseek-vl: towards real-world vision-language understanding. *arXiv preprint arXiv:2403.05525*, 2024.
- Lu, P., Bansal, H., Xia, T., Liu, J., Li, C., Hajishirzi, H., Cheng, H., Chang, K.-W., Galley, M., and Gao, J. Mathvista: Evaluating mathematical reasoning of foundation models in visual contexts. *arXiv preprint arXiv:2310.02255*, 2023.
- Luo, R., Zheng, Z., Wang, Y., Yu, Y., Ni, X., Lin, Z., Zeng, J., and Yang, Y. Ursa: Understanding and verifying chain-of-thought reasoning in multimodal mathematics. *arXiv preprint arXiv:2501.04686*, 2025.
- Masry, A., Do, X. L., Tan, J. Q., Joty, S., and Hoque, E. ChartQA: A benchmark for question answering about charts with visual and logical reasoning. In Muresan, S., Nakov, P., and Villavicencio, A. (eds.), *Findings of the Association for Computational Linguistics: ACL 2022*, pp. 2263–2279, Dublin, Ireland, May 2022. Association for Computational Linguistics.
- Miyai, A., Yang, J., Zhang, J., Ming, Y., Lin, Y., Yu, Q., Irie, G., Joty, S., Li, Y., Li, H., et al. Generalized out-of-distribution detection and beyond in vision language model era: A survey. *arXiv preprint arXiv:2407.21794*, 2024.
- Muja, M. and Lowe, D. G. Scalable nearest neighbor algorithms for high dimensional data. *IEEE Transactions on Pattern Analysis and Machine Intelligence*, 36(11): 2227–2240, 2014.
- OpenAI. GPT-4V(ision) system card, 2023. URL <https://openai.com/research/gpt-4v-system-card>.
- OpenAI. Learning to reason with llms, September 2024. URL <https://openai.com/index/learning-to-reason-with-llms/>.
- OpenAI. GPT-4o system card, 2024. URL <https://openai.com/research/gpt-4o-system-card>.
- Peng, S., Fu, D., Gao, L., Zhong, X., Fu, H., and Tang, Z. Multimath: Bridging visual and mathematical reasoning for large language models. *arXiv preprint arXiv:2409.00147*, 2024.
- Qi, Z., Ma, M., Xu, J., Zhang, L. L., Yang, F., and Yang, M. Mutual reasoning makes smaller llms stronger problem-solvers. *arXiv preprint arXiv:2408.06195*, 2024.
- Qiao, R., Tan, Q., Dong, G., Wu, M., Sun, C., Song, X., GongQue, Z., Lei, S., Wei, Z., Zhang, M., et al. We-math: Does your large multimodal model achieve human-like mathematical reasoning? *arXiv preprint arXiv:2407.01284*, 2024.
- Qwen Team. Qwen2.5: A party of foundation models, September 2024. URL <https://qwenlm.github.io/blog/qwen2.5/>.
- Roberts, D. and Roberts, L. Smart vision-language reasoners. *arXiv preprint arXiv:2407.04212*, 2024.
- Russell, S. and Wefald, E. Principles of metareasoning. *Artificial Intelligence*, 49(1):361–395, 1991. ISSN 0004-3702.
- Searle, J. R. Minds, brains, and programs. *Behavioral and brain sciences*, 3(3):417–424, 1980.
- Shi, W., Hu, Z., Bin, Y., Liu, J., Yang, Y., Ng, S.-K., Bing, L., and Lee, R. K.-W. Math-LLaVA: Bootstrapping mathematical reasoning for multimodal large language models. In *Findings of the Association for Computational Linguistics: EMNLP 2024*, pp. 4663–4680, Miami, Florida, USA, November 2024. Association for Computational Linguistics.
- Team, G., Anil, R., Borgeaud, S., Alayrac, J.-B., Yu, J., Soricut, R., Schalkwyk, J., Dai, A. M., Hauth, A., Millican, K., et al. Gemini: a family of highly capable multimodal models. *arXiv preprint arXiv:2312.11805*, 2023.
- Team, Q. Qvq: To see the world with wisdom, December 2024. URL <https://qwenlm.github.io/blog/qvq-72b-preview/>.
- Thawakar, O., Dissanayake, D., More, K., Thawkar, R., Heakl, A., Ahsan, N., Li, Y., Zumri, M., Lahoud, J., Answer, R. M., et al. Llamav-ol: Rethinking step-by-step visual reasoning in llms. *arXiv preprint arXiv:2501.06186*, 2025.
- Wang, K., Pan, J., Shi, W., Lu, Z., Ren, H., Zhou, A., Zhan, M., and Li, H. Measuring multimodal mathematical reasoning with MATH-vision dataset. In *The Thirty-eight Conference on Neural Information Processing Systems Datasets and Benchmarks Track*, 2024a.
- Wang, P., Bai, S., Tan, S., Wang, S., Fan, Z., Bai, J., Chen, K., Liu, X., Wang, J., Ge, W., et al. Qwen2-vl: Enhancing vision-language model’s perception of the world at any resolution. *arXiv preprint arXiv:2409.12191*, 2024b.
- Wang, P., Li, L., Shao, Z., Xu, R., Dai, D., Li, Y., Chen, D., Wu, Y., and Sui, Z. Math-shepherd: Verify and reinforce LLMs step-by-step without human annotations. In Ku, L.-W., Martins, A., and Srikumar, V. (eds.), *Proceedings of the 62nd Annual Meeting of the Association for Computational Linguistics (Volume 1: Long Papers)*, pp.

- 9426–9439, Bangkok, Thailand, August 2024c. Association for Computational Linguistics.
- Wang, P., Li, L., Shao, Z., Xu, R., Dai, D., Li, Y., Chen, D., Wu, Y., and Sui, Z. Math-shepherd: Verify and reinforce llms step-by-step without human annotations. In *Proceedings of the 62nd Annual Meeting of the Association for Computational Linguistics (Volume 1: Long Papers)*, pp. 9426–9439, 2024d.
- Wang, W., Chen, Z., Wang, W., Cao, Y., Liu, Y., Gao, Z., Zhu, J., Zhu, X., Lu, L., Qiao, Y., et al. Enhancing the reasoning ability of multimodal large language models via mixed preference optimization. *arXiv preprint arXiv:2411.10442*, 2024e.
- Wang, X., Wei, J., Schuurmans, D., Le, Q. V., Chi, E. H., Narang, S., Chowdhery, A., and Zhou, D. Self-consistency improves chain of thought reasoning in language models. In *The Eleventh International Conference on Learning Representations*, 2023.
- Wang, Y., Chen, W., Han, X., Lin, X., Zhao, H., Liu, Y., Zhai, B., Yuan, J., You, Q., and Yang, H. Exploring the reasoning abilities of multimodal large language models (mllms): A comprehensive survey on emerging trends in multimodal reasoning. *arXiv preprint arXiv:2401.06805*, 2024f.
- Wei, J., Wang, X., Schuurmans, D., Bosma, M., Xia, F., Chi, E., Le, Q. V., Zhou, D., et al. Chain-of-thought prompting elicits reasoning in large language models. *Advances in neural information processing systems*, 35:24824–24837, 2022.
- Wu, J., Feng, M., Zhang, S., Che, F., Wen, Z., and Tao, J. Beyond examples: High-level automated reasoning paradigm in in-context learning via mcts. *arXiv preprint arXiv:2411.18478*, 2024a.
- Wu, S., Peng, Z., Du, X., Zheng, T., Liu, M., Wu, J., Ma, J., Li, Y., Yang, J., Zhou, W., et al. A comparative study on reasoning patterns of openai’s o1 model. *arXiv preprint arXiv:2410.13639*, 2024b.
- Xu, G., Jin, P., Hao, L., Song, Y., Sun, L., and Yuan, L. Llava-o1: Let vision language models reason step-by-step. *arXiv preprint arXiv:2411.10440*, 2024.
- Yang, J., Dong, Y., Liu, S., Li, B., Wang, Z., Tan, H., Jiang, C., Kang, J., Zhang, Y., Zhou, K., et al. Octopus: Embodied vision-language programmer from environmental feedback. In *European Conference on Computer Vision*, pp. 20–38. Springer, 2025.
- Yang, Y., Ma, Y., and Liu, P. Weak-to-strong reasoning. In Al-Onaizan, Y., Bansal, M., and Chen, Y.-N. (eds.), *Findings of the Association for Computational Linguistics: EMNLP 2024*, pp. 8350–8367, Miami, Florida, USA, November 2024. Association for Computational Linguistics.
- Yao, H., Huang, J., Wu, W., Zhang, J., Wang, Y., Liu, S., Wang, Y., Song, Y., Feng, H., Shen, L., et al. Mulberry: Empowering mllm with o1-like reasoning and reflection via collective monte carlo tree search. *arXiv preprint arXiv:2412.18319*, 2024.
- Yao, S., Yu, D., Zhao, J., Shafran, I., Griffiths, T., Cao, Y., and Narasimhan, K. Tree of thoughts: Deliberate problem solving with large language models. In Oh, A., Naumann, T., Globerson, A., Saenko, K., Hardt, M., and Levine, S. (eds.), *Advances in Neural Information Processing Systems*, volume 36, pp. 11809–11822. Curran Associates, Inc., 2023.
- Ye, Q., Xu, H., Xu, G., Ye, J., Yan, M., Zhou, Y., Wang, J., Hu, A., Shi, P., Shi, Y., et al. mplug-owl: Modularization empowers large language models with multimodality. *arXiv preprint arXiv:2304.14178*, 2023.
- Ye, W., Liu, S., Kurutach, T., Abbeel, P., and Gao, Y. Mastering atari games with limited data. In Ranzato, M., Beygelzimer, A., Dauphin, Y., Liang, P., and Vaughan, J. W. (eds.), *Advances in Neural Information Processing Systems*, volume 34, pp. 25476–25488. Curran Associates, Inc., 2021.
- Yin, S., Fu, C., Zhao, S., Li, K., Sun, X., Xu, T., and Chen, E. A survey on multimodal large language models. *arXiv preprint arXiv:2306.13549*, 2023.
- Zeng, Z., Cheng, Q., Yin, Z., Wang, B., Li, S., Zhou, Y., Guo, Q., Huang, X., and Qiu, X. Scaling of search and learning: A roadmap to reproduce o1 from reinforcement learning perspective. *arXiv preprint arXiv:2412.14135*, 2024.
- Zhang, D., Li, J., Huang, X., Zhou, D., Li, Y., and Ouyang, W. Accessing gpt-4 level mathematical olympiad solutions via monte carlo tree self-refine with llama-3 8b. *arXiv preprint arXiv:2406.07394*, 2024a.
- Zhang, D., Zhou, S., Hu, Z., Yue, Y., Dong, Y., and Tang, J. Rest-mcts*: Llm self-training via process reward guided tree search. *Advances in Neural Information Processing Systems*, 2024b.
- Zhang, J., Huang, J., Jin, S., and Lu, S. Vision-language models for vision tasks: A survey. *IEEE Transactions on Pattern Analysis and Machine Intelligence*, 46(8):5625–5644, 2024c.
- Zhang, R., Wei, X., Jiang, D., Guo, Z., Li, S., Zhang, Y., Tong, C., Liu, J., Zhou, A., Wei, B., et al. Mavis: Mathematical visual instruction tuning with an automatic data engine. *arXiv preprint arXiv:2407.08739*, 2024d.

- Zhang, R., Zhang, B., Li, Y., Zhang, H., Sun, Z., Gan, Z., Yang, Y., Pang, R., and Yang, Y. Improve vision language model chain-of-thought reasoning. *arXiv preprint arXiv:2410.16198*, 2024e.
- Zhang, R., Jiang, D., Zhang, Y., Lin, H., Guo, Z., Qiu, P., Zhou, A., Lu, P., Chang, K.-W., Qiao, Y., et al. Math-verse: Does your multi-modal llm truly see the diagrams in visual math problems? In *European Conference on Computer Vision*, pp. 169–186. Springer, 2025.
- Zhang, X., Li, J., Chu, W., Hai, J., Xu, R., Yang, Y., Guan, S., Xu, J., and Cui, P. On the out-of-distribution generalization of multimodal large language models. *arXiv preprint arXiv:2402.06599*, 2024f.
- Zhang, Z., Zhang, A., Li, M., hai zhao, Karypis, G., and Smola, A. Multimodal chain-of-thought reasoning in language models. *Transactions on Machine Learning Research*, 2024g. ISSN 2835-8856.
- Zhou, A., Yan, K., Shlapentokh-Rothman, M., Wang, H., and Wang, Y.-X. Language agent tree search unifies reasoning, acting, and planning in language models. In *Forty-first International Conference on Machine Learning*, 2024.
- Zhu, D., Chen, J., Shen, X., Li, X., and Elhoseiny, M. Minigt-4: Enhancing vision-language understanding with advanced large language models. *arXiv preprint arXiv:2304.10592*, 2023.
- Zhuang, W., Huang, X., Zhang, X., and Zeng, J. Math-puma: Progressive upward multimodal alignment to enhance mathematical reasoning. *arXiv preprint arXiv:2408.08640*, 2024.
- Zong, Y. and Qiu, X. GAOKAO-MM: A Chinese human-level benchmark for multimodal models evaluation. In Ku, L.-W., Martins, A., and Srikumar, V. (eds.), *Findings of the Association for Computational Linguistics: ACL 2024*, pp. 8817–8825, Bangkok, Thailand, August 2024. Association for Computational Linguistics.

Appendix of AStar

This comprehensive supplementary material provides in-depth insights into our AStar method, covering additional descriptions, experimental details, and results. The appendix is organized as follows:

Table of Contents

A. Preliminaries

- A.1. Overall Notations
- A.2. MLLM Reasoning
- A.3. Monte Carlo Tree Search
- A.4. Verification Methods

B. Algorithm Details

- B.1. Action Space
- B.2. Reward Value in MCTS

C. More Details about Experimental Setup

- C.1. Benchmarks and Datasets
- C.2. Baselines
- C.3. Implementation Details

D. Supplementary Results

- D.1. Detailed Results on Multimodal Reasoning Benchmarks
- D.2. Comparison with Strong Baselines
- D.3. Integration with SFT
- D.4. Weak-to-Strong Generalization

E. Case Study

A. Preliminaries

This section describes overall notations (A.1), MLLM reasoning (A.2), monte carlo tree search (A.3), and verification methods (A.4).

A.1. Overall Notations

The definitions for notations are in Table 5.

A.2. MLLM Reasoning

With the advancement of computational resources and expanded datasets, MLLMs have demonstrated remarkable capabilities across various multimodal tasks (Yin et al., 2023; Zhang et al., 2024c; Wang et al., 2024f). These range from visual reasoning tasks like chart understanding and visual question-answering (Masry et al., 2022; Hartsock & Rasool, 2024) to more complex perception-action tasks in autonomous driving and robotics (Driess et al., 2023; Cui et al., 2024; Yang et al., 2025), where models must integrate visual inputs with decision-making processes. Central to these achievements is the development of effective reasoning methods, which can substantially enhance MLLM problem-solving capabilities, enabling even smaller models to achieve sophisticated reasoning abilities (Wang et al., 2024b; Dong et al., 2024a; Thawakar et al., 2025). To formalize this reasoning process, we consider an autoregressive pre-trained MLLM serving as a policy model π_θ . Given

Table 5. Notation Table

Character	Meaning
π_θ	policy MLLM
I	task instruction
\mathcal{D}_I	demonstration examples of I , which is ϕ in zero-shot settings
D_s	seed data
D_t	test data
x_t	multimodal test problem, consisting of input question q and images i
y_d	decoded answer
y_g	gold standard answer
y_t	reasoning trajectory / solution
T	number of reasoning steps
T_d	number of tokens in decoded answer y_p
a_t	t-th decoded answer token of y_d
s_t	t-th reasoning step of trajectory y_t
S_t	t-th state, which consists of input x and preceding reasoning steps $(s_1, s_2, \dots, s_{t-1})$
a_t	t-th action based on the previous state S_{t-1}
s	node s in the tree structure
p	parent node of s
$Q(s)$	reward value of node s
p_φ	process reward model
o_ψ	outcome reward model

an input problem x_t , the model generates a sequence $output = (s_0, s_1, s_2, \dots, s_T)$ through iterative token prediction, where $s_0 := x_t$ represents the initial state and s_T corresponds to the solution y_p . We define this generated sequence $(s_0, s_1, s_2, \dots, s_T)$ as a reasoning trajectory y_t . The conditional probability distribution of generating the complete reasoning trajectory is:

$$\pi_\theta(y_t, y_d | I, x_t, \mathcal{D}_I) = \underbrace{\prod_{t=1}^T \pi_\theta(s_t | s_{<t}, I, x_t, \mathcal{D}_I)}_{\text{Intermediate Reasoning Process}} \cdot \underbrace{\prod_{t=1}^{T_d} \pi_\theta(a'_t | a'_{<t}, y_t, I, x_t)}_{\text{Answer Decoding}}, \quad (5)$$

Following (Hao et al., 2023; Ge et al., 2024), we can conceptualize MLLMs as world models, with the complex reasoning process formulated as a Markov decision process. Specifically, when addressing complex reasoning challenges in real-world scenarios, at each time step t , the model receives a state S_{t-1} , comprising the original input problem x and preceding reasoning steps $(s_0, s_1, s_2, \dots, s_{t-1})$. The policy model π_θ then generates the current action $a_t = \pi_\theta(\Phi(S_{t-1}))$, which prompts the MLLM to produce the next reasoning step s_t . The entire process, from the initial step s_0 to the final output s_T , naturally forms a complete trajectory or chain of thought.

Inspired by recent advances in language model reasoning capabilities, researchers have explored OpenAI o1-like structured reasoning approaches to enhance long-chain reasoning in MLLMs. These approaches aim to develop systematic thinking patterns that enable models to perform complex multi-step reasoning. The process can be formalized under the following theoretical framework:

$$P_{\pi_\theta}(y_d = y_g | x_t) = \mathbb{E}_{(s_0, s_1, \dots, s_T) \sim P_{\pi_\theta}(y_t | x_t)} [P(y_d = y_g | s_0, s_1, \dots, s_T, x_t)] \quad (6)$$

where $P(y_d = y_g | s_0, s_1, \dots, s_T, x)$ represents the probability of obtaining an accurate final answer given the test problem x_t and reasoning trajectory y_t .

Early work explored multimodal chain-of-thought (CoT) (Zhang et al., 2024g), addressing the limitations of conventional MLLMs that typically defaulted to simple 'direct prediction' mode due to the scarcity of high-quality long-chain reasoning

Table 6. Method Comparison: Recent Multimodal Structured Reasoning Approaches.

Method	Open-Source Only	Data Volume	Training-Free	Training Cost ↓	Inference Cost ↓
AR-MCTS (Dong et al., 2024a)	✓	34.5K	✓	-	High
Mulberry (Yao et al., 2024)	✗	260K	✗	High	Low
LLaVA-CoT (Xu et al., 2024)	✗	100K	✗	High	Low
URSA (Luo et al., 2025)	✗	1100K	✗	High	Low
LlamaV-o1 (Thawakar et al., 2025)	✗	118K	✗	High	Low
AStar (Ours)	✓	0.5K	✓	Low	Low

data. However, these approaches often exhibit instability in multimodal reasoning tasks due to the distribution shift between training and inference (Wang et al., 2024e). Two primary methods have emerged to address this challenge: *explicit search mechanisms* and *teacher-guided distillation*. Recent advances in these approaches are summarized in Table 6.

(1) *Explicit search mechanisms.* These approaches leverage explicit search structures (e.g., Monte Carlo tree search, MCTS) with specialized reward models to guide the exploration of solution paths. AR-MCTS (Dong et al., 2024a) combines MCTS with active retrieval to expand the solution space and enhance performance, though its extensive iterations demand significant computational resources. Moreover, the quality and relevance of retrieved examples at each exploration step substantially impact model performance. Similarly, Mulberry (Yao et al., 2024) employs collective knowledge to enable collaborative conjecture, search, and identification of effective reasoning paths via MCTS. However, it requires substantial training data (260K samples) generated with expensive proprietary models, making it computationally intensive.

(2) *Teacher-guided distillation.* This approach focuses on distilling structured reasoning patterns through long-form CoT (Wei et al., 2022; Zhang et al., 2024g; Luo et al., 2025) instruction data, typically requiring supervision from proprietary models for data synthesis. For instance, LLaVA-CoT (Xu et al., 2024) explicitly structures visual reasoning into four stages (Summary, Caption, Reasoning, and Conclusion), utilizing 100K synthetic data samples for downstream task fine-tuning. Similarly, URSA (Luo et al., 2025) proposes a three-module data synthesis strategy integrating CoT distillation, trajectory rewriting, and format standardization, which relies on Gemini-Flash-002.

A.3. Monte Carlo Tree Search

As a heuristic search algorithm, MCTS has demonstrated remarkable success in complex reasoning and decision-making environments (Chaslot et al., 2008; Ye et al., 2021; Zhou et al., 2024). The algorithm conceptualizes search spaces as tree structures and has achieved significant breakthroughs across various domains, most notably in game-playing AI such as AlphaGo and AlphaZero (Dong et al., 2020). The basic MCTS algorithm involves an iterative search process with four key steps: selection, expansion, simulation, and backpropagation. As an example in multimodal mathematical reasoning, Figure 10 illustrates the four phases in an iteration, expanding the tree and then updating reward values.

Leveraging MCTS, recent approaches like AR-MCTS (Dong et al., 2024a) exploit MLLMs’ intrinsic capabilities and active retrieval for iterative exploration to enhance visual complex reasoning. However, these methods demand substantial computational resources due to extensive iterations. While approaches like Mulberry (Yao et al., 2024) attempt to integrate tree structures through model training, they require large-scale datasets and significant computational overhead. Moreover, current methods typically employ static reasoning processes, lacking the ability to adapt reasoning strategies based on problem complexity. In contrast, our approach employs MCTS only during the generation of prior reasoning patterns (referred to as “thought cards” in Sec. 3.2) and references these thought cards during inference to achieve efficient reasoning. This design enables AStar to adaptively match reasoning strategies to problem complexity, significantly reducing time complexity compared to traditional tree search methods while maintaining comprehensive search coverage and performance, thus achieving an optimal efficiency-effectiveness trade-off.

A.4. Verification Methods

After obtaining multiple valid candidate solutions for the test multimodal query $x_t = [q; i]$, selecting the most accurate reasoning trajectory among candidates presents a critical challenge. In multimodal reasoning, self-consistency (Wang et al., 2023) represents a simple yet effective approach, where the final answer is determined through majority voting among

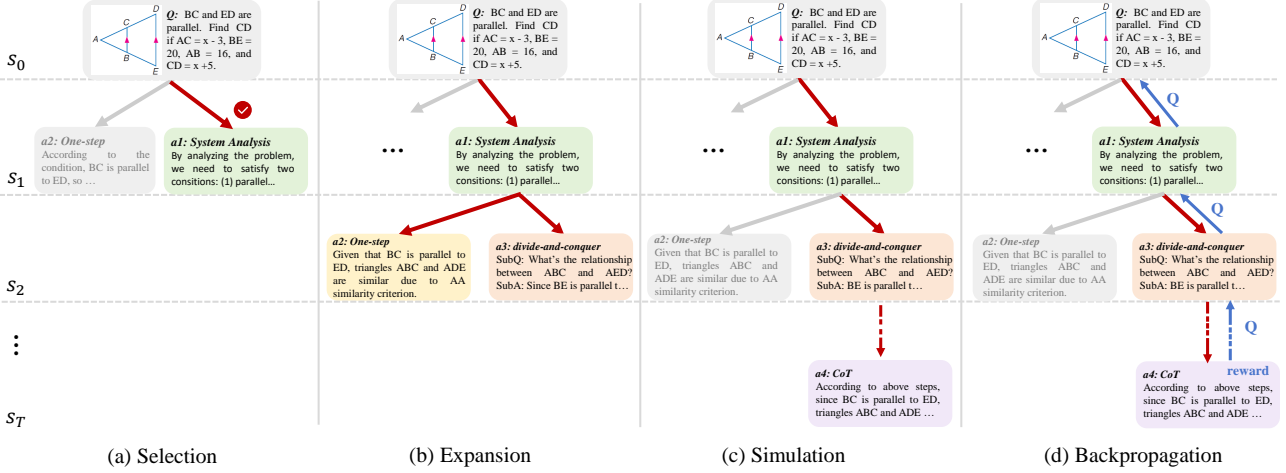


Figure 10. An illustration of the four phases in an iteration of MCTS for complex reasoning tasks (A.3).

sampled paths:

$$y^* = \arg \max_{y \in Y} \sum_{i=1}^m \mathbb{I}(y_i = y) \quad (7)$$

where Y denotes the set of all possible decoded answers, and \mathbb{I} is the indicator function. This strategy exploits the observation that a complex reasoning problem typically admits multiple valid reasoning paths leading to its unique correct answer. Thus, repeatedly sampled actions at the same state likely indicate successful task completion. However, for complex reasoning tasks where models may only achieve correct reasoning with low probability, simple self-consistency might not provide stable performance.

Recent advances in LLM reasoning verification have demonstrated significant improvements in reasoning capabilities through verification modules (Wang et al., 2024d; Zhang et al., 2024b). This has motivated the integration of outcome and process supervision in multimodal domains (Dong et al., 2024a; Luo et al., 2025) to enhance reasoning performance. However, the scarcity of multimodal supervision data and challenges in ensuring supervision signal quality often compromise verification effectiveness, with few high-performance open-source verification models currently available. Therefore, for simplicity, we leverage mature text-domain outcome reward models (ORM).

Specifically, in the text domain, given a text problem q and its reasoning trajectory y_t , ORM ($\mathcal{D} \times \mathcal{S} \rightarrow \mathbb{R}$) assigns a single real-value to indicate whether y_t is correct. ORM is usually trained with a cross-entropy loss (Cobbe et al., 2021; Li et al., 2023):

$$\mathcal{L}_{\text{ORM}} = y_g \log r_{y_t} + (1 - y_g) \log(1 - r_{y_t}) \quad (8)$$

where y_g is the golden answer ($y_g = 1$ if $traj$ is correct else $y_g = 0$), and r_{traj} is the sigmoid score of $traj$ assigned by ORM. The effectiveness of ORM heavily depends on training data quality. For reasoning problems with definitive answers, researchers can construct the ORM training set automatically by: (1) sampling candidate solutions, and (2) labeling solutions based on answer correctness. While this approach may introduce false positives (incorrect reasoning leading to correct answers), prior work has demonstrated its effectiveness in training robust ORM models (Lightman et al., 2024; Wang et al., 2024c). This enables the development of high-performing open-source verification models in the text domain.

To leverage these powerful text-domain verification models for visual reasoning while maintaining our principle of balancing performance and efficiency, we directly employ an MLLM to translate the original visual problems into pure text format.

$$q = \pi_{\theta}(x_t, \text{prompt}_{\text{translate}}) \quad (9)$$

where $\text{prompt}_{\text{translate}}$ denotes a translation prompt (e.g., “please translate the question and visual image into a pure text format”). The resulting text question q and the derived language-based reasoning steps derived from prior visual reasoning are then jointly processed by the ORM model for path selection and verification.

Table 7. Comparison with other search-based LLM and MLLM methods. Note that, most method contain limited space. In contrast, we define a rich set of reasoning actions, thus enhancing the upper bound of model reasoning capabilities.

Type	Method	Action Space
LLM	Tree-of-Thought (Yao et al., 2023)	a_3 : one-step thought
	RAP (Hao et al., 2023)	a_5 : divide and conquer
	ReST-MCTS* (Zhang et al., 2024b)	a_3 : one-step thought
	MCTSr (Zhang et al., 2024a)	a_4 : chain-of-thought, a_6 : self-reflection
MLLM	AR-MCTS (Dong et al., 2024a)	a_3 : one-step thought
	LLaVA-CoT (Xu et al., 2024)	a_4 : chain-of-thought
	URSA (Luo et al., 2025)	a_4 : chain-of-thought
	Ours	$a_1, a_2, a_3, a_4, a_5, a_6$

Our experiments indicate that this approach achieves improvements over simple self-consistency with minimal computational overhead. Future work could explore integration with high-quality verification models for potentially better results. In this paper, we utilize off-the-shelf ORM model: Llama3.1-8B-ORM-Mistral-Data¹.

B. Algorithm Details

B.1. Action Space

Reasoning capabilities are fundamental for handling diverse tasks, encompassing multiple cognitive dimensions. Prior work has categorized reasoning into deductive, inductive, abductive, and analogical approaches (Wang et al., 2024f). While open-source MLLMs demonstrate basic task competency, advanced models necessitate more sophisticated human-like reasoning abilities to achieve their full potential (Zeng et al., 2024). A key insight from recent studies suggests that model reasoning performance is bounded by their available reasoning actions (Wu et al., 2024b). Current frameworks, however, operate within a constrained action space (Table 7), which may limit the reasoning capabilities of MLLMs. To expand models’ reasoning capabilities beyond these constraints, we propose a comprehensive framework with six fundamental reasoning actions:

- *Visual Parsing* (a_1): Extracting and analyzing visual information from input images to support multimodal reasoning tasks.
- *System Analysis* (a_2): Analyzing the overall structure of the problem and identifying the constraints and conditions before addressing it, thereby clarifying task requirements effectively.
- *One-Step Thought* (a_3): Generating the next one-step thought based on the given question and the preceding reasoning steps.
- *Chain-of-Thought* (a_4): Facilitating step-by-step reasoning by constructing a logical sequence of intermediate thoughts, where each step incrementally builds on the previous ones.
- *Divide and Conquer* (a_5): Breaking down a complex reasoning problem into several smaller subproblems and progressively solving them to achieve the overall solution.
- *Self-Reflection* (a_6): Engaging in timely reflection of prior solutions and implementing necessary refinement during the reasoning process to ensure accuracy.

¹<https://huggingface.co/RLHFlow/Llama3.1-8B-ORM-Mistral-Data>

Table 8. Comparison with other search-based LLM and MLLM methods. Note that, most method contain limited space. In contrast, we define a rich set of reasoning actions, thus enhancing the upper bound of model reasoning capabilities.

Type	Dataset	Evaluation Dimensions
Visual Question Answering	ChartQA (Masry et al., 2022)	chart understanding and reasoning
	MMStar (Chen et al., 2024b)	6 core capabilities, like scientific reasoning
Mathematics	MathVista (Lu et al., 2023)	12 core capabilities, like arithmetic reasoning
	MathVerse (Zhang et al., 2025)	6 distinct versions-text-dominant
	MathVision (Wang et al., 2024a)	16 mathematical domains
Commonsense and science	GAOKAO-MM (Zong & Qiu, 2024)	8 subjects, like history

B.2. Reward Value in MCTS

To simplify the construction of thought cards via the MCTS iteration, we avoid introducing an external reward model to score each step. Given the current skepticism regarding the self-rewarding capabilities of language models, alternative methods are necessary. Inspired by the principle that actions leading to correct answers should be rewarded more frequently, we aim to increase their likelihood of selection in future MCTS tree expansions. Following (Zhou et al., 2024; Wu et al., 2024a), we define the reward value as the likelihood (or confidence) of self-consistency via majority voting. Note that this principle applies only to leaf nodes. The Q-values of intermediate nodes are initially set to 0 and are dynamically updated during the backpropagation process, as described in Equation 1.

C. More Details about Experimental Setup

C.1. Benchmarks and Datasets

Here are the details of the benchmarks used in our experiments. The statistics of the datasets are recorded in Table 8. Note that the evaluation metrics for all datasets are consistent with their official standards, primarily focusing on accuracy.

- **ChartQA** (Masry et al., 2022) is a comprehensive benchmark for chart-based question answering that emphasizes visual and logical reasoning capabilities. The dataset comprises 9,608 human-authored questions and 23,111 machine-generated questions derived from human-written chart summaries. It incorporates 20,882 real-world charts from diverse sources including Statista, Pew Research, Our World in Data, and OECD, spanning multiple domains and visualization styles. ChartQA addresses prior dataset limitations through its focus on human-authored questions, real-world charts, and open-vocabulary responses. We utilize this dataset to evaluate our method’s performance on visual chart question-answering tasks commonly encountered in real-world scenarios.
- **MMStar** (Chen et al., 2024b) serves as a vision-critical multimodal benchmark for evaluating MLLM capabilities. It addresses two fundamental limitations in existing evaluations: the redundancy of visual inputs and potential training data contamination. Comprising 1,500 meticulously curated challenge samples across six core competencies and 18 evaluation axes, the benchmark undergoes rigorous validation to ensure visual necessity and minimal data leakage. We employ this comprehensive dataset to assess our method’s general reasoning capabilities.
- **MathVista** (Lu et al., 2023) is a mathematical visual benchmark consisting of 6,141 examples. These examples are divided into two subsets: *testmini* with 1,000 annotated examples and *test* comprising 5,141 problems without public answers. We conduct our evaluation on the *testmini* subset to assess visual comprehension and compositional reasoning capabilities.
- **MathVerse** (Zhang et al., 2025) is a comprehensive and specialized visual mathematics benchmark for assessing multimodal mathematical reasoning capabilities of MLLMs. The benchmark contains 2,612 visual math problems, combining 1,236 newly collected problems from public repositories with 1,376 problems from existing benchmarks. Human annotators have transformed each problem into six distinct versions-text-dominant, text-lite, text-only, vision-intensive, vision-dominant, and vision-only—each offering different levels of multimodal information. We utilize this dataset to evaluate AStar’s performance across varying degrees of multimodal integration.

- **MathVision** (Wang et al., 2024a) constitutes a meticulously compiled collection of 3,040 mathematics problems, each incorporating visual elements from authentic mathematics competitions. The dataset spans 16 mathematical domains and features a five-tier difficulty classification system. We employ this dataset to evaluate our model’s performance on challenging reasoning tasks.
- **GAOKAO-MM** (Zong & Qiu, 2024) represents a multimodal evaluation framework derived from the Chinese National College Entrance Examination (Gaokao). It encompasses eight academic subjects and includes twelve categories of images, such as diagrams, function graphs, maps, and photographs. The benchmark aims to evaluate models’ abilities to understand and reason over diverse multimodal content, reflecting the complexity and breadth of knowledge. We leverage this dataset to assess AStar’s cross-domain generalization capabilities.

C.2. Baselines

We evaluate AStar against four strong baseline categories:

Open-source general MLLMs: Recent advances include Qwen2-VL (Wang et al., 2024b) and InternVL2 (Chen et al., 2024d), which demonstrate exceptional capabilities in complex reasoning and mathematical problem-solving.

Open-source math MLLMs: Several models have been specifically optimized for mathematical reasoning in MLLMs. These models can be grouped based on their core methodologies:

1. Dataset Construction and Fine-Tuning:

- a. G-LLaVA (Gao et al., 2023): Introduces the Geo170K dataset, comprising over 170K geometric image-caption and question-answer pairs, to enhance MLLMs’ geometric problem-solving capabilities.
- b. Math-LLaVA (Shi et al., 2024): Develops the MathV360K dataset by collecting 40K high-quality images with question-answer pairs and synthesizing an additional 320K pairs, then fine-tunes the LLaVA-1.5 model to improve multimodal mathematical reasoning.
- c. MultiMath (Peng et al., 2024): Constructs the MultiMath-300K dataset, encompassing K-12 level mathematical problems with image captions and step-wise solutions, and trains the MultiMath-7B model to bridge visual and mathematical reasoning.

2. Progressive Alignment and Curriculum Learning:

- a. Math-PUMA (Zhuang et al., 2024): Proposes a three-stage Progressive Upward Multimodal Alignment methodology to enhance MLLMs’ mathematical reasoning skills, focusing on aligning visual and textual modalities through a structured training process.
- b. LlamaV-o1 (Thawakar et al., 2025): Introduces a multimodal visual reasoning model trained using a multi-step curriculum learning approach, organizing tasks progressively to facilitate incremental skill acquisition and problem-solving.

3. CoT Reasoning Integration:

- a. LLaVA-CoT (Xu et al., 2024): Develops a vision-language model designed to conduct autonomous multistage reasoning, employing a structured approach that includes summarization, visual interpretation, logical reasoning, and conclusion generation.
- b. URSA (Luo et al., 2025): Proposes a three-module synthesis strategy integrating CoT distillation, trajectory-format rewriting, and format unification, resulting in the MMathCoT-1M dataset and the URSA-7B model, which demonstrates state-of-the-art performance on multiple multimodal mathematical benchmarks.

4. Large-Scale Multimodal Pre-Training:

- a. InfiMM-Math (Han et al., 2024): Introduces InfiMM-WebMath-40B, a high-quality dataset comprising 24 million web pages, 85 million associated image URLs, and 40 billion text tokens, aiming to improve MLLMs’ mathematical reasoning through large-scale multimodal pre-training.

5. Slow-Thinking System Implementation:

- a. Virgo (Du et al., 2025): Explores a straightforward approach to implementing multimodal slow-thinking systems by fine-tuning a capable MLLM with a small amount of textual long-form thought data, demonstrating that such reasoning processes can be effectively transferred to MLLMs.

Advanced closed-source MLLMs: Leading proprietary models including GPT-4V (OpenAI, 2023), GPT-4o (OpenAI, 2024), and Gemini-1.5-Pro (Team et al., 2023) demonstrate exceptional capabilities in multimodal understanding and task-solving, setting benchmarks for open-source alternatives.

Multimodal tree-based methods: Recent works incorporate explicit search mechanisms into multimodal reasoning. AR-MCTS (Dong et al., 2024a) enhances reasoning by combining Monte Carlo Tree Search (MCTS) with active retrieval, improving reasoning space diversity and reliability. Mulberry (Yao et al., 2024) leverages multi-model collaboration through MCTS’s four iterative operations (selection, expansion, simulation, backpropagation) to identify optimal reasoning paths.

C.3. Implementation Details

We utilize the vLLM framework² with the following parameters: temperature set to 0.8, top p set to 0.9, and max tokens set to 1024. All experiments were conducted on a machine running Ubuntu 22.04, equipped with NVIDIA A100-80GB GPUs. We list all hyperparameters in Table 9.

Table 9. All hyperparameters utilized in this paper.

Hyperparameter	Value	Description
temperature	0.8	vllm inference settings
top-p	0.9	
top-k	40	
repetition penalty	1.0	
max tokens	1024	
maximum tree depth d_{max}	5	MCTS
exploration weight w	2.0	
predefined terminal threshold c	0.90	
balance factor k	0.95	VOC-based optimal path selection in Sec. 3.2 Phase 2

In the MCTS-powered prior thought card construction stage, we implement an early termination strategy based on self-consistency (Wang et al., 2023) for enhanced efficiency. Building on the observation that repeated action sampling at the same state often indicates successful task completion, we terminate simulation early when the model’s consistency score exceeds a threshold c (i.e., $SC(s) > c$).

In the inference stage, we evaluate AStar’s effectiveness across both LLM and MLLM architectures. For MLLMs, we can directly utilize their native visual understanding and reasoning capabilities for visual parsing. For traditional LLMs like Qwen2.5-7B, we employ Qwen2-72B-VL solely for visual information extraction, deliberately avoiding its visual reasoning capabilities. This design choice ensures that the inference backbone remains the primary reasoning component while maintaining computational efficiency.

D. Supplementary Results

This section presents supplementary results and analysis, including: D.1 Detailed Results on Multimodal Reasoning Benchmarks, D.2 Comparison with Strong Baselines, D.3 Integration with SFT, and D.4 Weak-to-Strong Generalization.

²<https://github.com/vllm-project/vllm>

D.1. Detailed Results on Multimodal Reasoning Benchmarks

We provide detailed test results based on various mathematical abilities using the MathVista benchmark. As shown in Table 10, AStar demonstrates notable strengths in statistics and challenging logic, whereas other models exhibit superior performance in algebraic and geometric problem-solving. Notably, with Qwen2-VL-2B as our inference backbone, our 2B model even surpasses larger models such as InternLM-XComposer2-VL-7B and Math-LLaVA, achieving performance comparable to GPT-4V. This indicates that, regardless of model size, our AStar reasoning framework effectively enhances multimodal reasoning capabilities.

Table 10. Results on MathVista *testmini* detailed mathematics capabilities. The best results of closed-source MLLMs are highlighted in green. The best and second-best results of open-source MLLMs are highlighted in red and blue respectively.

Model	#Params	ALL	ALG	ARI	GEO	LOG	NUM	SCI	STA
<i>Baselines</i>									
Random Choice	-	17.9	25.8	13.8	22.7	13.4	8.8	15.8	14.3
Human Performance	-	60.3	50.9	59.2	51.4	40.7	53.8	64.9	63.9
<i>Closed-source MLLMs</i>									
Qwen-VL-Plus (Bai et al., 2023)	-	43.3	39.1	32.0	39.3	18.9	26.4	59.0	56.1
GPT-4V (OpenAI, 2023)	-	49.9	53.0	49.0	51.0	21.6	20.1	63.1	55.8
<i>Open-source General MLLMs</i>									
mPLUG-Owl2-7B (Ye et al., 2023)	7B	22.2	23.6	19.2	23.9	13.5	12.7	26.3	21.4
LLaVA-1.5-13B (Liu et al., 2024b)	13B	25.7	19.6	28.6	17.6	10.8	27.8	33.6	22.9
MiniGPT-v2 (Chen et al., 2023)	7B	23.1	28.1	21.0	24.7	16.2	16.7	25.4	17.9
InternLM-XComposer2-VL-7B (Dong et al., 2024c)	7B	47.8	32.0	51.6	30.5	13.5	43.8	37.7	62.8
SPHINX-MoE (Lin et al., 2023)	8× 7B	42.3	31.7	41.6	30.5	16.2	27.1	50.8	50.8
DeepSeek-VL (Lu et al., 2024)	7B	34.9	29.2	38.8	27.2	18.9	43.1	35.3	33.2
InternVL2-8B (Chen et al., 2024d)	8B	58.3	59.8	56.4	60.3	10.8	30.6	59.0	68.8
Qwen2-VL (Wang et al., 2024b)	7B	58.9	44.1	57.5	43.1	24.3	41.7	66.4	75.1
<i>Open-source Math MLLMs (Large-Scale Training)</i>									
G-LLaVA (Gao et al., 2024)	7B	25.1	36.0	19.4	37.6	15.2	17.7	21.0	15.1
Math-LLaVA (Shi et al., 2024)	13B	46.6	51.5	40.7	56.2	23.3	34.7	47.7	42.3
Multimath-7B (Peng et al., 2024)	7B	50.0	61.9	42.2	64.9	23.3	32.6	42.6	49.2
Math-PUMA-Qwen2-7B (Zhuang et al., 2024)	7B	47.9	47.7	46.2	47.3	21.6	32.6	42.6	55.8
URSA-7B (Luo et al., 2025)	7B	59.8	74.0	53.5	77.4	21.6	35.4	58.2	57.1
AStar (Ours, Training-free Reasoning)	7B	63.5	69.0	63.1	71.7	61.3	60.0	48.2	68.8
	2B	49.6	51.0	49.9	53.1	34.7	46.8	41.3	54.3

D.2. Comparison with Strong Baselines

Table 11 provides a performance comparison of our method against leading open-source and closed-source models. AStar with a 7B inference backbone achieves competitive performance with larger MLLMs. Notably, on the challenging MathVision dataset, our approach exhibits substantial improvements. This suggests that while simpler visual tasks may not significantly benefit from structured reasoning strategies—with performance primarily determined by model capacity—our method shows increasing performance advantages on more complex datasets like MathVerse and MathVision, surpassing both InternVL2.5-26B and InternVL2-Llama3-76B models despite their larger parameter counts of 26B and 72B respectively.

We also benchmark our approach against recent powerful multimodal reasoning methods, including LLaVA-CoT (Xu et al., 2024) and Virgo (Du et al., 2025). As shown in Table 12, comparative experiments across different model scales demonstrate that our AStar reasoning framework, which effectively integrates MLLMs’ inherent reasoning capabilities with external reasoning guidelines, achieves superior performance with minimal prior data. On challenging datasets like MathVerse, our method exhibits substantial improvements, with the 2B model achieving comparable performance to the extensively trained Virgo 7B model. Further analysis reveals two key insights: First, methods relying on vast solution spaces often struggle to identify appropriate reasoning paths, analogous to finding a needle in a haystack. Second, approaches dependent on

large-scale training data typically face difficulties in fully capturing complex long-chain reasoning patterns through implicit learning. In contrast, our method adaptively identifies suitable reasoning strategies based on problem complexity, enabling efficient inference across diverse scenarios.

Table 11. Comparison with leading LLMs. The best results are highlighted in **bold**. Results for off-the-shelf models are sourced from corresponding official websites.

Model	MathVista	MathVerse	MathVision	Average
<i>Closed-Source Models</i>				
GPT-4o-0513 (OpenAI, 2024)	63.8	50.2	30.4	48.2
GPT-4V (OpenAI, 2023)	49.9	54.4	24.8	43.1
Gemini-1.5-Pro (Team et al., 2023)	63.9	35.3	19.2	39.5
Claude-3.5-Sonnet (Anthropic, 2024)	67.7	-	-	-
Qwen-VL-Plus (Bai et al., 2023)	43.3	21.3	10.8	25.2
<i>Open-Source Models</i>				
Qwen2-VL-72B (Wang et al., 2024b)	70.5	-	25.9	-
LLaVA-OneVision-72B (Li et al., 2024)	67.5	39.1	-	-
InternVL2.5-26B (Chen et al., 2024d)	67.7	40.1	28.0	45.3
InternVL2-Llama3-76B (Chen et al., 2024d)	65.5	42.8	23.7	44.0
Astar (Ours)	63.5	54.0	32.4	50.0

Table 12. Comparison with recent works targeting enhanced multimodal reasoning through structured thinking. We list 2B and $\geq 7B$ -scale baselines. The best results in each box are highlighted in **bold**. Our method demonstrates significant performance improvements.

Model	Size	MMStar	ChartQA	MathVista	MathVerse
<i>2B-Scale Baselines</i>					
Mulberry (Yao et al., 2024)	2B	51.3	77.7	51.7	-
Astar (Ours)	2B	51.7	78.3	49.6	33.7
<i>$\geq 7B$-Scale Baselines</i>					
Insight-V (Dong et al., 2024d)	7B	61.5	81.5	59.9	-
AR-MCTS (Dong et al., 2024a)	7B	-	-	64.1	-
Mulberry (Yao et al., 2024)	7B	61.3	83.9	63.1	-
LLaVA-CoT (OpenAI, 2024)	11B	57.6	-	54.8	-
LlamaV-o1 (Thawakar et al., 2025)	11B	59.6	-	54.4	-
URSA (Luo et al., 2025)	7B	-	-	59.8	45.7
Virgo (Luo et al., 2025)	7B	-	-	-	37.5
Astar (Ours)	7B	61.7	83.9	63.5	54.0

D.3. Integration with SFT

To evaluate the versatility of the AStar framework, we conducted experiments on both pretrained base models and their supervised fine-tuning (SFT) counterparts. Table 13 presents a comprehensive comparison of model performance across different configurations. Our results demonstrate that the AStar framework consistently yields substantial improvements over the zero-shot performance reported in the original papers, regardless of whether it is applied to pretrained or SFT models.

Table 13. Integration With SFT on MathVision. We evaluate the AStar framework using Qwen2-VL-2B and Qwen2-VL-7B as backbone models, comparing both pre-trained base models and SFT variants across different difficulty levels.

Backbone	1	2	3	4	5	Average
Qwen2-VL-2B-Base	20.8	20.7	21.4	17.8	10.2	18.2
Qwen2-VL-2B	25.0	20.0	15.6	16.7	17.6	22.3
Qwen2-VL-7B-Base	26.8	20.6	23.7	26.7	22.4	23.4
Qwen2-VL-7B	26.5	21.3	26.2	29.8	23.8	25.2

Notably, the combination of SFT and AStar achieves superior performance, suggesting a synergistic effect between supervised fine-tuning and our framework. For instance, with Qwen2-VL-2B as the backbone, the SFT variant (Qwen2-VL-2B-Instruct) achieves better average performance (22.3% vs 18.2%) and shows particular strength in handling problems at difficulty levels 1 and 5, where it achieves 25.0% and 17.6% accuracy, respectively. Similarly, the Qwen2-VL-7B model with AStar demonstrates robust performance across all difficulty levels, achieving an average accuracy of 25.2%. These findings suggest promising future research directions for further integrating SFT techniques into the AStar framework to enhance overall system performance.

D.4. Weak-to-Strong Generalization

As described in (Bansal et al., 2024; Yang et al., 2024), interactions between weak and strong models can be categorized into three primary paradigms: 1) weak-to-strong improvement, where models with limited capabilities can effectively guide the development of more advanced models, 2) self-improvement, wherein the weak and strong models are identical, focusing on designing methods to enhance the model’s own performance, and 3) knowledge distillation, which involves transferring the capabilities or knowledge from strong models to weak models. Through our main results, where thought cards are constructed based on Qwen2-VL-7B, we have already demonstrated the significant potential of our AStar method in knowledge distillation (Qwen2-VL-7B → Qwen2-VL-2B) and self-improvement (Qwen2-VL-7B → Qwen2-VL-7B).

Therefore, in this section, we empirically evaluate AStar’s effectiveness in weak-to-strong generalization. We hypothesize that a weaker model, when integrated with AStar, can effectively guide a more powerful policy model. To test this hypothesis, we leverage the reasoning guidance (thought cards) generated by Qwen2-VL-7B to assist GPT-4o in solving challenging problems from the MathVision dataset.

As illustrated in Figure 11, we present a comprehensive comparison between GPT-4o’s zero-shot performance and its performance when enhanced with AStar (using Qwen2-VL-7B’s reasoning guidance) across multiple dimensions of the MathVision benchmark. Our results demonstrate that incorporating our reasoning paradigm enables models with limited capabilities to provide valuable supervision to stronger policy models. Notably, the Qwen2-VL-7B model, despite its relatively limited capabilities, successfully guides the more powerful, closed-source GPT-4o. This finding validates the potential of learning from prior reasoning patterns and offers promising insights for developing more scalable and sophisticated strategies to enhance AI reasoning capabilities.

E. Case Study

Taking a geometry problem in MathVerse as an example, we provide a qualitative comparison of LLaVA-NeXT-8B (Liu et al., 2024b), Qwen2-VL-7B (Wang et al., 2024b), and AStar-7B in Figure 12. The results demonstrate that LLaVA-NeXT-8B and Qwen2-VL-7B struggle to accurately parse complex geometric relationships, leading to potential errors in each step of their reasoning processes. In contrast, our AStar framework effectively combines MLLMs’ internal implicit reasoning capabilities with external explicit reasoning guidelines. This integration exhibits explicit and well-defined reasoning steps with comprehensive understanding, ultimately arriving at the correct solution.

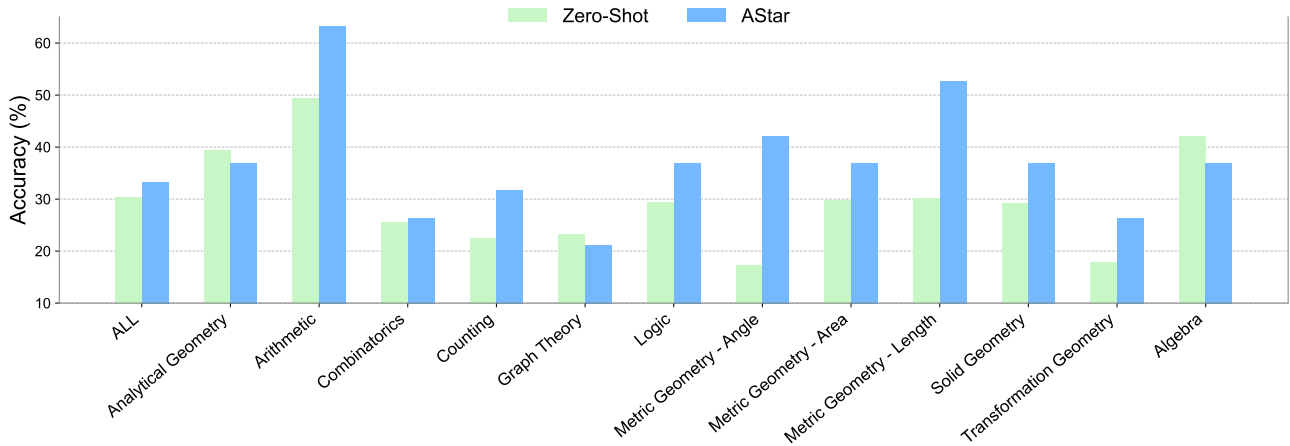


Figure 11. Weak-to-strong generalization results: Performance comparison of GPT-4o in zero-shot and AStar-enhanced (Qwen2-VL-7B guidance) settings across various dimensions of MathVision. The results demonstrate that a weaker model (Qwen2-VL-7B) can effectively guide a stronger model (GPT-4o) through the AStar framework, validating the framework’s potential for weak-to-strong generalization in mathematical reasoning tasks.

Requirement: Please answer the question and provide the option number, e.g. A, B, C, D at the end.

Question: In the figure shown above, the cylinder has radius of 3. If all the water in the rectangular container is poured into the cylinder, the water level rises from \$h\$ inches to \$(h+x)\$ inches. Which of the following is the best approximation of the value of \$x\$?

Choices:
 (A) 3
 (B) 3.4
 (C) 3.8
 (D) 4.2

Correct Answer: (D)

Solid Geometry

LLaVA:

We know that the volume of the cylinder changes when the rectangular prism’s water is transferred into it. The initial volume of water in the rectangular prism is $5 \times 6 \times 4 = 120$ cubic units. The volume of water in the cylinder after transferring the rectangular prism’s water is $3\pi(9)(h + x)$. Since we don’t know the exact amount of water transferred, we cannot determine the exact value of x without additional information such as the height of the water column in the cylinder after transferring the rectangular prism’s water or a specific relationship between the height of the water column and the depth of the cylinder. However, the question does not provide enough information to determine the value of x directly. Therefore, based on the given options, none of them provide the exact value of x .

The answer is: ❌

AStar

Step 1: Visual Parsing
 The image illustrates a transformation from a sector of a circle to a conical (bottomless) cap: The image shows two 3D geometric shapes, a cylinder on the left and a rectangular prism (cuboid) on the right. Both appear to be partially filled with a shaded substance, presumably water.

- Left Image: Cylinder
 - A vertical open-top cylinder.
 - Shaded region at the bottom represents the water.
 - Two dashed lines within the water show different water levels.
 - “ h ” marks the initial water level height.
 - “ x ” marks the additional height the water rises.
 - The radius of the cylinder is labeled as 3.
- Right Image: Rectangular Prism
 - A rectangular prism with a base that appears to be a rectangle.
 - Partially filled with water.
 - The water level is 4, the base is a rectangle with side lengths of 6 and 5.

Step 2: One-Step Thought
 Use the formula for the volume of a rectangular prism, $V = lwh$, where l is length, w is width, and h is height. Here, $V = 6 \times 5 \times 4 = 120$ cubic units.

Step 3: Chain-of-Thought
 Based on previous thinking, let’s think step by step:

- From Step 2, we know that the volume of the rectangular prism is $V = 120$ cubic units.
- The volume of the water in the cylinder is initially $V = \pi(r^2)h$, where $r = 3$ units (radius of the cylinder), and h is the initial height of the water. The volume of the water in the cylinder after transferring the water from the rectangular prism is $V = \pi \times (r^2) \times (h+x)$, where $h + x$ is the new height of the water in the cylinder.
- Given that the volume of the water increases due to the transfer, we set up the equation based on the volumes:

$$\pi \times (3^2) \times x = 120$$
- Simplifying further, we obtain:

$$9\pi x = 120$$

Solving for x :

$$x = 120 / 9\pi \approx 120 / 28.27 \approx 4.24$$

Therefore, the closest option is (D) 4.2. The answer is: ✅

Figure 12. Qualitative comparison of reasoning processes across different models. AStar demonstrates superior understanding through its explicit, well-structured reasoning steps, leading to accurate solution derivation. The comparison highlights AStar’s ability to systematically decompose complex geometric relationships while maintaining reasoning clarity throughout the problem-solving process.